JRC Scientific and Technical Reports

Integrated Modeling of Fate and Effects of Persistent Organic Pollutants in Marine Ecosystems

J. M. Zaldívar, D. Marinov, S. Dueri, I. Puillat, R. Carafa, N. Berrojalbiz, S. Lacorte, E. Jurado and J. Dachs

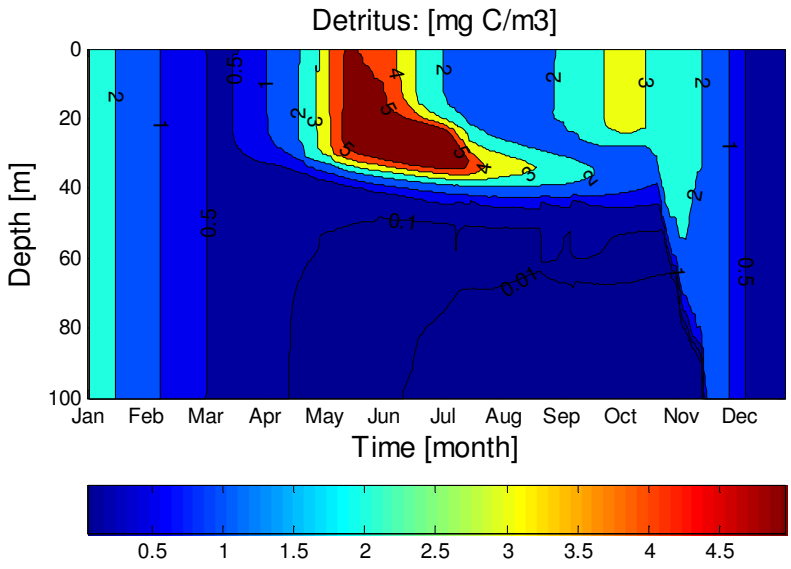

EUR 22882 EN - 2007

JRC
EUROPEAN COMMISSION

The mission of the JRC is to provide customer-driven scientific and technical support for the conception, development, implementation and monitoring of EU policies. As a service of the European Commission, the JRC functions as a reference centre of science and technology for the Union. Close to the policy-making process, it serves the common interest of the Member States, while being independent of special interests, whether private or national.

European Commission
Joint Research Centre

Contact information
Address: Via E. Fermi 1, TP 272
E-mail: jose.zaldivar-comenges@jrc.it
Tel.: +39-0332-789202
Fax: +39-0332-785807

http://www.jrc.ec.europa.eu

JRC 38014

EUR 22882 EN
ISBN 978-92-79-06662-7
ISSN 1018-5593

Luxembourg: Office for Official Publications of the European Communities

Printed in Italy

Table of Contents

List of Tables

List of Figures

1. Introduction

Contaminants reach surface waters through different pathways, ranging from atmospheric deposition, infiltration in the soil during heavy rainfalls and migration with the groundwater or transport in particulate and dissolved phase in rivers. Domestic and industrial sewage water represents a major global source of pollution for surface water. Furthermore, agricultural activities may be associated to the input of pesticides, while municipal and medical waste incinerators as well as industrial combustion processes can release chemical byproducts to the atmosphere. Normally, a mixture of contaminants is present in transitional, coastal as well as marine waters affecting their ecosystems.

When dealing with pollutants it is important to understand for a given compound its persistence (P) in the environment and its long range transport potential (LRTP). These two characteristics help in assessing its environmental fate as well as the spatial and temporal extents of environmental exposure (Leip and Lammel, 2004). Furthermore, it is also essential to identify the contamination sources and emissions. These have important implications for their fate as well as for the approach it should be followed to develop monitoring programs. For example, contaminants may be released in a pulse due to an accidental discharge; they may be periodically driven by human activities (application of pesticides in agriculture) or by environmental fluctuations (e.g. temperature dependence), or constantly during the year.

Even though the effects of contaminants are more pronounced in inland, transitional and coastal waters, the oceans play an important role in controlling the environmental transport, fate and sinks of organic pollutants, specifically persistent organic pollutants (POPs), at regional and global scales (Wania and Mackay, 1996; Dachs et al., 2002). It has been demonstrated that water-column processes have a strong impact on the air-sea exchange of organic contaminants, since their efficient removal from the mixed surface water layer reduces the volatilization rates and captures atmospheric pollutants (Dachs et al., 1999; Scheringer et al., 2004). Nevertheless, there is a complex interplay of processes controlling the vertical transport of contaminants in the water column the knowledge of which is limited due to the scarcity of measurements on the role of the ecosystems on the uptake, depuration and settling of POPs (Schulz-Bull et al., 1988; Dachs et al., 1997; Gustafsson et al., 1997; Dachs et al., 1999). On the other hand, coastal and marine sediments have been hypothesized to become a pool of contaminants available for mixing throughout the water column, especially during poorly stratified periods (Baker et al., 1991; Berlung et al., 2001; Bodgan et al., 2002; Ko et al., 2003; Jurado et al., 2007). Therefore, in

order to be able to simulate properly the dynamics of organic pollutants in the water column, we need to consider all these aspects, in particular for shallow water bodies and the ocean shelf zone.

The traditional approach to model contaminants in the water column is to consider two well-mixed boxes during stratification periods and one well-mixed the rest of the time (Schwarzenbach et al., 2003; Meijer et al., 2006). The extensive number of 0D models for these hydrophobic organic compounds (Wania and Mackay, 1996; Scheringer et al., 2000; Dalla Valle et al., 2003; Dueri et al., 2005) contrasts with the lack of spatially and temporally resolved models, with the exception of the recently developed coastal lagoon model for herbicides (Carafa et al., 2006), but its chemical behavior differs from those of POPs, and the lately one for HCH by Ilyina et al. (2006). In two previous works (Jurado et al., 2007; Marinov et al., 2007), we have developed a 1D dynamic hydrodynamic-contaminant model to analyze the influence of vertical mixing on the distribution of POPs in the water column. The effect of seasonal dynamics of phytoplankton on POPs fate has been also considered but as a forcing function. The selection of 1D model version followed two reasons – first, we planned to validate it using water column data for the selected chemicals and, second, the 1D version is adequate for open-sea areas, where the atmospheric transport is the prevalent route for the introduction of contaminants (Tolosa et al, 1997). Furthermore, the 1D approach avoids the difficulties associated with providing time-series of boundary conditions; it reduces computation time and prepares a simpler model variant which after verification gives the option to easily extend it to 3D model version using the COHERENS framework as it has been foreseen in Stream 4 for the Thau lagoon case study. The model was applied to the organic contaminants families selected in Thresholds, i.e. PCBs, PAHs, and PBDEs, plus dioxins and furans, PCDD/Fs.

In this work, we have introduced a food-web ecological model that considers phytoplankton, zooplankton, bacteria and detritus. The model uses nutrient concentrations as forcings and it has been validated using chlorophyll a data at two different stations in the Mediterranean. The dynamics of the ecosystem has been coupled with the previous develop fate model in terms of organic matter and partitioning of the POPs. Environmental concentrations in all ecological compartments are simulated. In order to perform a first validation of the coupled model, experimental data on PAHs obtained at the Finokalia Station, Island of Crete, Greece. (Tsapakis et al., 2005 and 2006) have been used (the validation will continue by incorporating all available experimental data from Thresholds' campaigns). The results show that the model is able to reproduce the experimental concentrations as well as the measured fluxes.

Notwithstanding, due to the low concentrations of PAHs in the considered remote area environment, the toxic effect model also developed in this work has not been validated now. However, the mesocosm experiments (D4.3.1 and D4.3.2) aiming at elucidate the combined effects of nutrient and contaminants are being used to validate this part of the model. These results will be an object of a further deliverable: D4.3.4.

At this end, once validated the integrated model will serve for the development of scenarios, making analysis of possible environmental thresholds or the assessment of plausible human pressure that could produce regime shifts. Thau lagoon (France) will work for a selected case study.

2. FOOD WEB MODEL

2.1. FOOD WEB STRUCTURE

In order to simulate the toxic effects of contaminants in marine ecosystems as well as the effects of the biological pump on the dynamics of contaminants a simplified model, following the analysis of data from mesocosm experiments conducted by NERI, has been developed. This model was considered as the minimum model able to deal with experimental observed effects in mesocosm experiments (Dahllöf and Hjorth, 2006) as well as to the analyze the variability (diurnal/nocturnal) of Persistent Organic Pollutants (POPs) found during the Mediterranean Cruise and in previous campaigns (Jaward et al., 2004).In the model (Fig. 2.1), phytoplankton are represented by two groups typifying diatoms and flagellates whereas zooplankton are also divided into two groups representing microzooplanton (< 200 µm) and mesozooplankton (0.2-2 mm). In addition, the microbial loop is also considering by modelling bacteria and detritus.

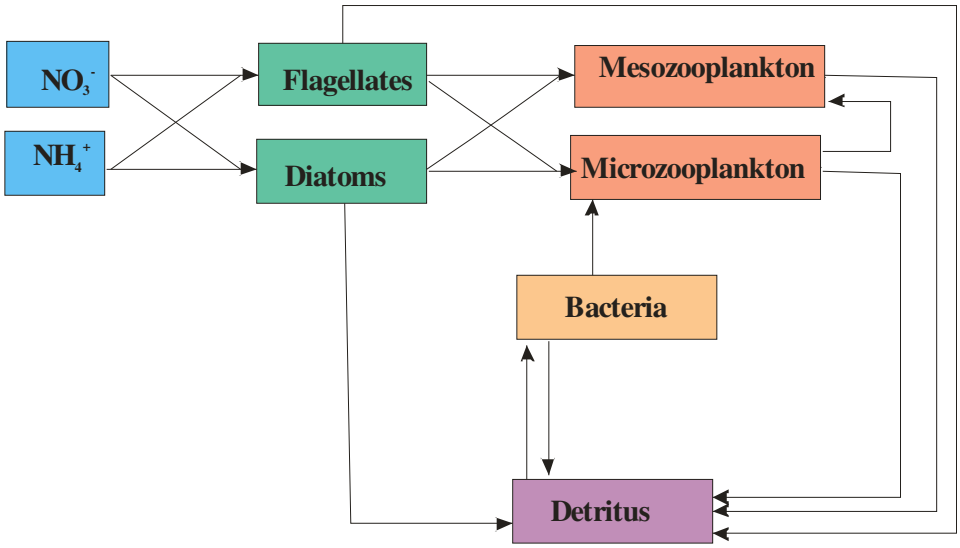

Figure 2.1. Simplified flow diagram in the marine ecosystem.

2.2. ECOLOGICAL MODEL DESCRIPTION

A schematic flow diagram of the marine ecosystem is summarised in Fig. 2.1. Besides the presence of nitrate and ammonium acting as nutrients in the water column (in this first formulation we have not considered the nutrient dynamics since we were interested in analysing the food wed dynamics), the model accounts for two types of phytoplankton: diatoms and flagellates (*Pd, Pf*), and two types of zooplankton: microzooplankton and mesozooplankton (*Zs, Zl*). In addition the model contains the so

called microbial loop, which accounts for the mineralization of dead organic mater, called detritus (*D*), performed by the bacteria (*B*). The ordinary differential equations may be written as:

$$\frac{dPd}{dt} = growth_{Pd} \cdot Pd - grazing_{Pd}^{Zs} \cdot Zs - grazing_{Pd}^{Zl} \cdot Zl - m_{Pd} \cdot Pd \quad (1)$$

$$\frac{dPf}{dt} = growth_{Pf} \cdot Pf - grazing_{Pf}^{Zs} \cdot Zs - grazing_{Pf}^{Zl} \cdot Zl - m_{Pf} \cdot Pf \quad (2)$$

$$\frac{dZs}{dt} = \left(grazing_{Pd}^{Zs} + grazing_{Pf}^{Zs}\right) \cdot eff_P \cdot Zs + grazing_B^{Zs} \cdot eff_B \cdot Zs - grazing_{Zs}^{Zl} \cdot Zl - excre_{Zs} \cdot Zs - m_{Zs} \cdot Zs^2 \quad (3)$$

$$\frac{dZl}{dt} = \left(grazing_{Pd}^{Zl} + grazing_{Pf}^{Zl}\right) \cdot eff_P \cdot Zl + grazing_{Zs}^{Zl} \cdot eff_{Zs} \cdot Zl - excre_{Zl} \cdot Zl - m_{Zl} \cdot Zl^2 \quad (4)$$

$$\frac{dB}{dt} = growth_B \cdot B - kd_B \cdot B - grazing_B^{Zs} \cdot Zs \quad (5)$$

$$\frac{dD}{dt} = mort_{\det} + unassim_{\det}^{P} + unassim_{\det}^{Z} + unassim_{\det}^{B} - upt_B - \beta \cdot D - w_s \cdot D \quad (6)$$

2.2.1. Phytoplankton (*Pf* and *Pd* in mmol N m^{-3})

Phytoplankton growth is modelled as the product of the maximum specific growth rate times an overall limitation function as:

$$growth_{Px} = \mu_{\max}^{Px} \cdot \min[f_1(I), f_2(T), f_3(NO_3^-, NH_4^+)] \quad (7)$$

where the maximum growth rate is 0.0625 h^{-1} for diatoms and 0.0417 h^{-1} for flagellates, respectively (Oguz et al., 1999).

The light limitation is parameterized according to Jassby and Platt (1976) by

$$f_1(I) = \tanh[a_p \cdot I(z,t)] \quad (8)$$

$$I(z,t) = I_s \cdot \exp[-(k_{water} + k_{phy}[Pf + Pd]) \cdot z] \quad (9)$$

where a_p (a_p = 0.01 m^2 W^{-1}) denotes the photosynthetic quantum efficiency parameter controlling the slope of *f(I)* versus the irradiance curve and I_s denotes the surface intensity of the PAR (photosynthetically active irradiance) taken as half of the incoming solar radiation. k_{water} is the extinction coefficient of the sea water (k_{water}= 0.08 m^{-1}) and k_{phy} is the phytoplankton self-shading coefficient (k_{phy}= 0.07 m^2/mmol N). In present application the I_s (W m^{-2}), PAR, has been taken from the Adriatic Sea 1D model run that was developed in Deliverable 2.6.2. Similarly, to run this 0D version, the temperature has been also taken from the surface temperature of the same1D model.

The temperature limitation function for phytoplankton is based on Lancelot *et al*. (2002)

$$f_2(T) = \exp\left[-\left(\frac{T - T_{opt}}{T_{width}}\right)^2\right] \tag{10}$$

with T_{opt} and T_{width} being the optimal temperature and the range of suitable temperatures respectively. In this case for diatoms: T_{opt}=16.5 ºC and T_{width}=7.5 ºC, whereas for flagellates T_{opt}=22.0 ºC and T_{width}=12.0 ºC.

The nutrient limitation is the sum of ammonium and nitrate limitation:

$$f_3(NO_3^-, NH_4^+) = f_a(NO_3^-) + f_b(NH_4^+) \tag{11}$$

where the limitations are expressed by the Michaelis-Menten uptake formulation:

$$f_a(NO_3^-) = \frac{[NO_3^-]}{K_{no} + [NO_3^-]} \cdot \exp(-\psi[\bar{NH_4}]) \tag{12}$$

$$f_b(NH_4^+) = \frac{[NH_4^+]}{K_{nh} + [NH_4^+]} \tag{13}$$

where K_{no}=0.5 mmol N m^{-3} and K_{nh}= 0.2 mmol N m^{-3} are half saturation constants for nitrate and ammonium uptake, respectively, and the exponent in Eq. (12) represents the inhibiting effect of ammonium concentration on nitrate uptake with ψ=3 m^3 mmol N^{-1} (Wrobleski, 1977).

The mortality of phytoplankton is expressed as a linear function of its biomass with m_{Pd}=1.67 10^{-3} h^{-1} and m_{Pf}= 3.33 10^{-3} h^{-1}, respectively.

2.2.2. Zooplankton (*Zs* and *Zl* in mmol N m^{-3})

In a similar way as in Oguz et al. (1999), we define the total food availability for each zooplankton group as:

$$F_{Zs} = b_{Pf} \cdot Pf + b_{Pd} \cdot Pd + b_B \cdot B \text{ and } F_{Zl} = a_{Pf} \cdot Pf + a_{Pd} \cdot Pd + a_{Zs} \cdot Zs \tag{14}$$

where a_{Pf}, a_{Pd}, a_{Zs} (0.3,0.8,0.7) and b_{Pf}, b_{Pd}, b_B (0.7,0.2,0.5) are the food preference coefficients. Grazing rates of microzooplankton are then defined as:

$$grazing_{Pd}^{Zs} = g_{\max}^{Zs} \frac{b_{Pd} \cdot Pd}{K_G + F_{Zs}} \tag{15}$$

$$grazing_{Pf}^{Zs} = g_{\max}^{Zs} \frac{b_{Pf} \cdot Pf}{K_G + F_{Zs}} \tag{16}$$

$$grazing_{B}^{Zs} = g_{maz}^{Zs} \frac{b_{B} \cdot B}{K_G + F_{Zs}} \tag{17}$$

where K_G is an apparent half saturation constant (K_G =0.5 mmol N m^{-3}) and $g_{\max}^{Zs}$ is the maximum grazing rate which is defined as a function of temperature as:

$$g_{\max}^{Zs} = g_{Zs}^{'} \exp\left[-\left(\frac{T - T_{opt}}{T_{width}}\right)^2\right] \quad (18)$$

with T_{opt} and T_{width} being the optimal temperature and the range of suitable temperatures, respectively. In this case for microzooplankton:T_{opt}=23.0 ºC and T_{width}=8.0 ºC. The maximum specific grazing rate for microzooplankton is g_{Zs}'= 0.036 h^{-1}.

The grazing rates of mesozooplankton are then defined as:

$$grazing_{Pd}^{Zl} = g_{\max}^{Zl} \frac{a_{Pd} \cdot Pd}{K_G + F_{Zl}} \quad (19)$$

$$grazing_{Pf}^{Zl} = g_{\max}^{Zl} \frac{a_{Pf} \cdot Pf}{K_G + F_{Zl}} \quad (20)$$

$$grazing_{Zs}^{Zl} = g_{\max}^{Zl} \frac{a_{Zs} \cdot Zs}{K_G + F_{Zl}} \quad (21)$$

where K_G is an apparent half saturation constant (K_G =0.5 mmol N m^{-3}) and $g_{\max}^{Zl}$ is the maximum grazing rate which is defined as a function of temperature as:

$$g_{\max}^{Zl} = g_{Zl}^{'} \exp\left[-\left(\frac{T - T_{opt}}{T_{width}}\right)^2\right] \quad (22)$$

with T_{opt} and T_{width} being the optimal temperature and the range of suitable temperatures respectively. In this case for mesozooplankton: T_{opt}=23.0 ºC and T_{width}=8 ºC. The maximum specific grazing rate for mesozooplankton is g_{Zs}'=0.033 h^{-1}.

The excretion rates, $excre_{Zs}$ and $excre_{Zl}$, are equal to $2.92 \cdot 10^{-3}$ h^{-1}. Following Oguz et al. (1999) the mortality terms are expressed in the quadratic form as suggested by Steele and Henderson (1992), with m_{Zs}=$1.67 \cdot 10^{-3}$ h^{-1} and m_{Zl} = $3.33 \cdot 10^{-3}$ h^{-1}, respectively. The assimilation coefficients eff_P, eff_{Zs} and eff_B are equal to 0.75.

*2.2.3. **Bacteria*** (B in mmol N m^{-3})

Bacterial growth represents a fraction of detritus uptake:

$growth_B = Y_B \cdot upt_B$

where Y_B=0.2 and bacterial uptake is defined as:

$$upt_B = b_{\max} \frac{D}{K_D + D} B \tag{23}$$

where K_D is the half saturation value for detritus uptake, K_D=25 mg C m^{-3} and b_{max} is the maximum uptake rate of detritus by bacteria that depends on temperature as:

$$b_{\max} = b'_{\max} \exp\left[-\left(\frac{T - T_{opt}}{T_{width}} \right)^2 \right] \tag{24}$$

with T_{opt} and T_{width} being the optimal temperature and the range of suitable temperatures respectively. In this case for bacteria: T_{opt}=30.0 ºC and T_{width}=18 ºC. The maximum specific growth rate for bacteria is $b'_{\max}$ =0.4 h^{-1}. Bacterial lysis is defined as: $kd_B \cdot B$, with kd_B=0.01 h^{-1}.

2.2.4. Detritus

Phytoplankton, zooplankton and bacteria mortalities plus fecal pellets, constitute the unassimilated part of ingested food, contribute to the detritus compartment. Detritus due to mortality is expressed as:

$$mort_{\det} = \left(m_{Pd} \cdot Pd + m_{Pf} \cdot Pf \right) \cdot CN_P + \left(m_{Zs} \cdot Zs^2 + m_{Zl} \cdot Zl^2 \right) \cdot CN_Z + kd_B \cdot B \tag{25}$$

where CN_P and CN_Z are ratios of mg C/mmol N for phytoplankton and zooplankton, respectively. CN_P=48, CN_Z =63. The other component consists on the unassimilated part of ingested food by zooplankton, that can be written as:

$$unassim^P_{\det} = (1 - eff_p) \cdot (grazing^{Zs}_{Pd} + grazing^{Zs}_{Pf}) \cdot Zs \cdot CN_P + (1 - eff_P) \cdot (grazing^{Zl}_{Pd} + grazing^{Zl}_{Pf}) \cdot Zl \cdot CN_P \tag{26}$$

$$unassim^Z_{\det} = (1 - eff_Z) \cdot grazing^{Zl}_{Zs} \cdot Zl \cdot CN_Z \tag{27}$$

$$unassim^B_{\det} = (1 - eff_B) \cdot grazing^{Zs}_{B} \cdot Zs \cdot CN_B \tag{28}$$

where CN_B is the ratio of mg C/mmol N for bacteria, CN_B=48. The other two terms in the mass balance for detritus account for the mineralization and for the settling, with a detritus decomposition rate β=4.17 10^{-3} h^{-1} and a sinking velocity w_s=8.33 10^{-2} m h^{-1}.

2.3. 0D SIMULATED RESULTS

The model was run for several years to analyze the results before incorporating it into the spatially resolved structure using temperature and solar radiation data sets obtained from the 1D model, see fig. 2.2. Nutrient concentrations were kept constant during all year with values of $[NO_3^-]$=1 mmol N m^{-3} and $[NH_4^+]$=0.11 mmol m-^{3}. Figure 2.3 shows an example of the results obtained considering surface water (depth 0.5 m).

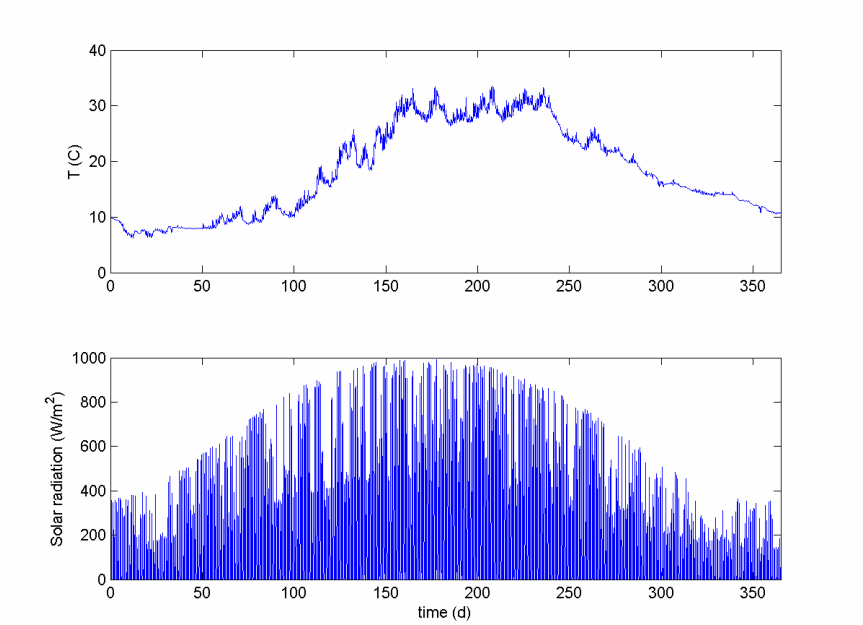

Figure 2.2. Temperature and solar radiation used as forcing in the 0D ecological model.

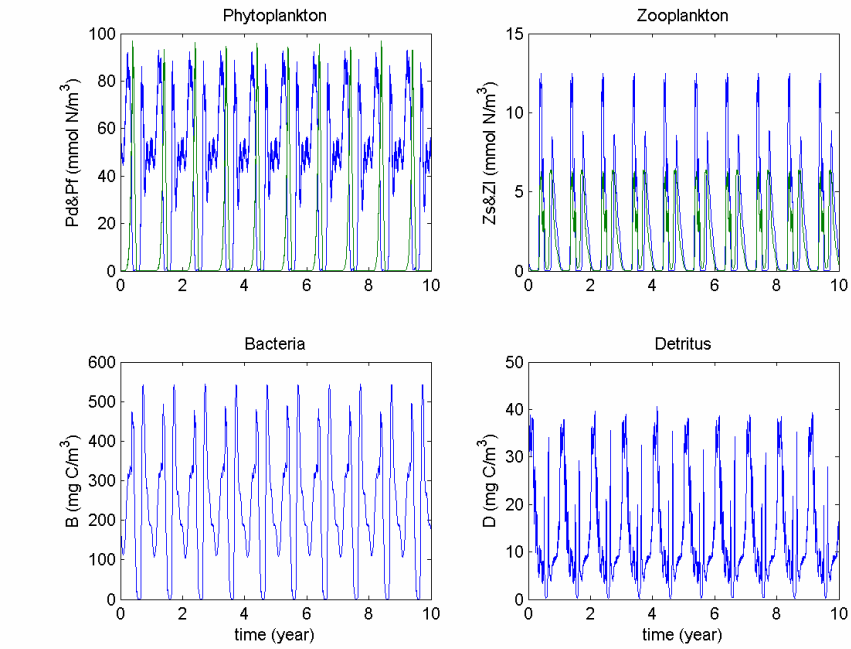

Figure 2.3. Simulated annual variations of the compartments in the model.

The model produced reasonable results in this 0D implementation. However, all biomasses were more typical of a coastal zone than that of the open sea. This was due to the high and constant level of nutrients considered during the year and the fact that there was no depletion during spring and summer. Besides, as shown in Fig.2.3 the model predicts a remarkable seasonality in concentrations of

phytoplankton, zooplankton, bacteria and detritus that obviously has an influence on POP occurrence and fate. Discussion on this issue could be found later in the validation part of the model.

3. Bioaccumulation model

3.1. PARTITIONING BEHAVIOUR OF CONTAMINANTS IN BIOTA

3.1.1. Bioconcentration

The bioconcentration factor (BCF) of a compound is defined as the ratio of concentration of the chemical in the organism and in water at equilibrium.

$$BCF = \frac{C_i}{C_w} \tag{29}$$

The uptake of a chemical from water is a passive diffusion process across the skin or gill membrane, similar to oxygen uptake. Bioconcentration is related to the octanol-water partition coefficient of the compound and the lipid fraction in tissues of the organism (Van der Oost *et al*., 2003).

Boese *et al*. (1984) demonstrated a significant correlation between the accumulation of contaminants in the body of the organism and lower levels of oxygen in the water. Furthermore less hydrophobic compounds (with lower K_{ow}) show smaller uptake rates.

Some experiments have been carried out to measure constants of uptake, manly using fish and lipophilic chemicals like PCBs, HCBs etc.; e.g. Vigano *et al*. (1994) measured in rainbow trout a time range between 15 and 256 days to reach equilibrium after exposure to different concentrations of PCBs. Several log-linear correlations exist between the logarithm of the octanol-water partition coefficient and the BCF. (e.g.: Devillers *et al*., 1996; Hawker and Connel, 1985). Thomann (1989) demonstrated that the depuration rate inversely correlated to the logarithm of the K_{ow}.

3.1.2. Biomagnification

The biomagnification factor is defined as the ratio between the uptake of a contaminant from food and its removal (Sijm *et al*., 1992),

$$BMF = \frac{K_{food}}{K_{dep} + K_{ecx} + K_{meta}} \tag{30}$$

The uptake from food can be also defined as:

$$K_{food} = F_F \cdot eff_F \tag{31}$$

where F_F is the quantity of food ingested per unit mass per unit time and eff_F is the efficiency of uptake of the chemical from food. Nevertheless, the biomagnification factor is not sufficient to account for all accumulation of contaminants in aquatic organisms.

Russell *et al*. (1999) demonstrated that significant biomagnification is not observed for values of log K_{ow} lower than 5.5; Fisk *et al*. (1998) drew similar conclusions: chemicals with log $K_{ow} \approx 7$ show a high potential to accumulate along aquatic food webs.

Gobas *et al*. (1988) explained the process of biomagnification with a fugacity-based hypothesis: the transport of chemical is led by a difference in fugacity (from high to low fugacity compartments). In other laboratory experiments Gobas *et al*. (1999) demonstrated that digestibility and absorption of food are critical parameters controlling the BCFs in fish.

Furthermore Opperhuizen (1991) found that biomagnification accounts for a more important fraction of accumulation of chemicals for larger fish than for smaller fish; this might be due to decrease in gill ventilation volume whereas the relative feeding rate is almost the same.

3.1.3. Bioaccumulation

Transfer mechanisms of persistent hydrophobic contaminants in aquatic organisms are essentially two: the first one is the direct uptake of dissolved phase from water trough skin or gills, named bioconcentration, the second one is the indirect uptake of bound contaminants to suspended particular matter and through consumption of contaminated food (biomagnification).

The bioaccumulation of pollutants may be an important source of hazard for the ecosystem, due to adverse effect not quickly evident (e.g. acute or chronic toxicity) but that became manifested after years in the higher levels of the trophic food web or in a later stage of life of organisms or after several generations (Van der Oost *et al*., 2003).

The mass balance of a contaminant (A) in the tissue of an aquatic organism can be defined as (adapted from Thomann, 1989 and Thomann *et al*., 1992):

$$\frac{dC_i}{dt} = k_{upt} C_A^{diss} + k_{food} C_{food} - k_{dep} C_i - k_{meta} C_i - k_G C_i \qquad (32)$$

where the first two terms indicate the uptake of contaminant from water and predation, respectively, and the third, fourth and fifth terms indicate losses of contaminants through depuration (release from gill membranes or excretion through feces), metabolism and dilution effect of growth, respectively.

3.1.4. Biotransformation

Removal of chemicals in an aquatic organism is realized essentially through two main pathways: the contaminant is either eliminated by depuration/excretion in the original chemical form (parent molecule) or bio-transformed by the organism.

The latter process leads in general to the formation of more hydrophilic compounds. In this case the metabolites are rapidly excreted after a detoxification reaction. These compounds are normally less harmful than the parent compound. However, in some cases the parent compound can be "bioactivated" through metabolic reactions and lead to formation of a metabolite more toxic than the former molecule (Van der Oost, *et al.,* 2003).

The organ most involved in the detoxification reaction is the liver, and metabolic-specific reactions are directly linked to the toxic activity of a chemical in the body and to its half-life (Vermeulen, 1996).

The velocity and efficiency of metabolic clearance have been demonstrated to be a function of several species-specific characteristics: presence of enzymes, feeding status, stage of life, spawning period (Van der Oost *et al.*, 2003).

Organisms in the aquatic environment are readily exposed to chemical mixtures, and risk assessment has therefore to account for the occurrence of diverse contaminants with different toxic potentials. However, the toxic effects of pollutants in mixture may not simply be additive but can be synergistic or antagonistic as well.

The identification of relevant contributors to observed mixture effects in site-specific assessments would offer a scope for measures targeted at toxicity reduction, which is of particular interest for costly remediation efforts (Altenburger *et al.*, 2004). Realistically, the testing of all chemical mixtures and possible environmental concentrations is not viable. As a consequence, different models on mixture toxicity based on the toxicity of single compounds have been developed. The objective is to reduce the amount of experiments and to be able to predict mixtures toxicity. However, the main draw back associated with this approach is the attribution of a correct mechanism/mode of action to the involved chemicals (Maciel and Zaldívar, 2005).

3.2. MODEL FORMULATION

For simplicity, let us assume a certain contaminant. In this case we have taken PAHs as the selected family, because certain members, e.g. pyrene and PAHs mixtures have been investigated within the Thresholds project. However, the model has a general scope and can be extended to other contaminants. We assume that the concentrations of the PAH compound in the dissolved phase is calculated using the fate model developed in Deliverable 2.6.2 after solving the mass balance equations that gives the total concentration in the water column. The model considers the contaminant as dissolved, attached to dissolved organic carbon and to particulate organic matter. In this case, we consider only the concentration in the dissolved phase as bioavailable for the organism.

3.2.1. Bioconcentration in phytoplankton and bacteria

Bioconcentration of contaminants by phytoplankton can be calculated assuming constant uptake and depuration rates and by modelling the water-phytoplankton exchange as shown by Del Vento and Dachs (2002).

The concentration of a chemical in the two phytoplankton groups (C_{Pd} ,C_{Pf}) and for bacteria (C_B) over time can be expressed using Eq. (32), assuming there is no biomagnification (k_{food}= 0), a self-sustained phytoplankton community (k_G= 0), and a metabolism rate much lower than the depuration rate. Under these assumptions Eq. (32) becomes:

$$\frac{dC_{Pd}}{dt} = k_{upt}^{Pd} \cdot C_{PAH}^{dis} - k_{dep}^{Pd} \cdot C_{Pd} \tag{33}$$

$$\frac{dC_{Pf}}{dt} = k_{upt}^{Pf} \cdot C_{PAH}^{dis} - k_{dep}^{Pf} \cdot C_{Pf} \tag{34}$$

$$\frac{dC_{B}}{dt} = k_{upt}^{B} \cdot C_{PAH}^{dis} - k_{dep}^{B} \cdot C_{B} \tag{35}$$

where k_{upt} (m^3 ng^{-1} h^{-1}) and k_{dep} (h^{-1}) are the uptake and depuration rates constants. Bacteria feed on detritus. However, it is assumed that there is no egestion and therefore we do not consider the concentration in the particulate phase (Detritus).Uptake and depuration constants can be parameterized as function of bioconcentration factors of the chemical, permeability (P, m/h) of the cell membrane and specific surface area (S_p, m^2/kg) (Del Vento and Dachs, 2002):

$$\begin{aligned} k_{dep} &= \frac{S_p \cdot P}{BCF} \\ k_{upt} &= S_p \cdot P \end{aligned} \tag{36}$$

The specific surface area of phytoplankton has been estimated by assuming oblate ellipsoid shape for flagellates and cylinder shape for diatoms, taking into account the shapes of the dominant species of each class in the Adriatic Sea: (*Prorocentrum minimum* (Fig. 3.1) for flagellates and *Skeletonema costatum* for diatoms)(Regione Emilia Romagna, 2002). In particular the volume (V_f) and surface area (A_f) of flagellates are given by:

$$\begin{aligned} V_f &= \frac{4}{3}\pi abc \\ A_f &= 4\pi \cdot \left(\frac{a^p b^p + a^p c^p + b^p c^p}{3} \right)^{1/p} \end{aligned} \tag{37}$$

where a, b and c are the lengths of the three semi-axes, determining the shape of the ellipsoid and p ≈ 1.6075 (Knud Thomsen's formula).The lengths of a, b and c have been set equal to 18, 12.5 and 12.5

µm (http://www.nmnh.si.edu/botany/projects/dinoflag/Taxa/Pminimum.htm). Diameters of diatoms cells and pervalvaraxis are taken as of 11.5 µm of diameter and 31.5 µm of height respectively (http://elvire.antajan.chez-alice.fr/Diatoms/Skeletonema.html). The density of phytoplankton (ρ_{phyto}) is taken as of 1025 Kg/m^3 (Del Vento and Dachs, 2002). This gives a volume of $1.18 \cdot 10^{-14}$ m^3 and $3.27 \cdot 10^{-15}$ m^3, areas of $2.56 \cdot 10^{-9}$ and $1.35 \cdot 10^{-9}$ m^2, and specific surface areas (*Sp*) of 211.57 and 401.29 m^2 kg^{-1}, respectively.

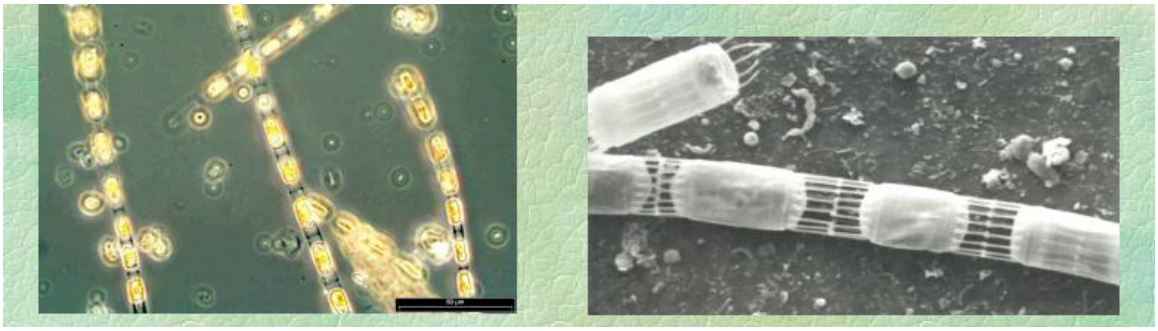

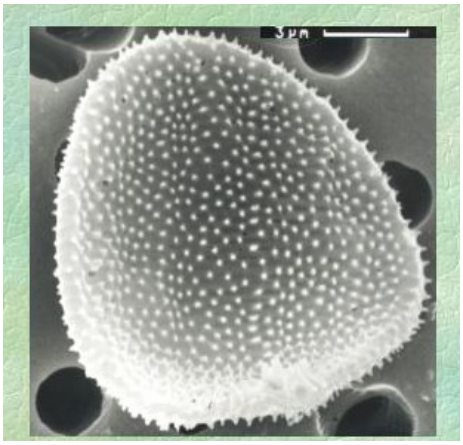

Figure 3.1. Picture of main phytoplankton species considered for the Adriatic Sea: *Prorocentrum minimum* (on the left) and *Skeletonema costatum* (on the top).

Bioconcentration of contaminants in bacteria has been calculated in the same way and the specific surface area (S_p) has been calculated assuming a diameter of 1 µm, spherical shape and density (ρ_{bac}) equal to 1080 kg m^{-3} (Hailiang *et al.*, 2002), which gives 2777.78 m^2 kg^{-1}.

In order to predict uptake and depuration rates it is necessary to know values for BCF and P. Since estimations of BCF and P exist only for a few number of compounds (e.g. Skoglund et al., 1996; Wallberg and Andersson, 1999; Swackhamer and Skoglund. 1993), these parameter has been calculated using empirical approximation based on the physical-chemical properties of the contaminant.

It has been demonstrated (Swackhamer and Skoglund, 1993; Stange and Swackhamer, 1994) that, for many organic compounds, the logarithm of the bioconcentration factor plotted against the logarithm of the octanol/water partition coefficient gives two linear correlations (with a plateau in correspondance to

log $K_{ow} \approx 6.5$, that can be fitted by least squares and may be represented by the following log linear equations (Del Vento and Dachs, 2002):

$$\log BCF = 1.085 \log K_{ow} - 3.770 \quad \text{for } \log K_{ow} < 6.4 \tag{38}$$

$$\log BCF = 0.343 \log K_{ow} + 0.913 \quad \text{for } \log K_{ow} \geq 6.4 \tag{39}$$

The same considerations can be made for the estimation of permeability of cell membrane and similar regressions have been proposed (Del Vento and Dachs, 2002):

$$\log P = 1.340 \log K_{ow} - 8.433 \quad \text{for } \log K_{ow} < 6.4 \tag{40}$$

$$\log P = 0.078 \quad \text{for } \log K_{ow} \geq 6.4 \tag{41}$$

Table 3.1 summarizes the uptake and depuration constants used in Eqs. (33)-(35) to calculate the concentrations of PAHs in diatoms, flagellates and bacteria.

Table 3.1. Uptake ($m^3 \cdot kg^{-1} \cdot d^{-1}$) and depuration ($d^{-1}$) constants used in the model.

Compound (PAHs)	**log K_{ow}**	**Diatoms (*Pd*)**		**Flagellates (*Pf*)**		**Bacteria (*B*)**	
		k_{upt}	k_{dep}	k_{upt}	k_{dep}	k_{upt}	k_{dep}
Naphthalene	3.37	0.0486	0.0631	0.0256	0.0333	0.336	0.436
Fluorene	4.12	0.491	0.0979	0.259	0.0517	3.400	0.678
Antracene	4.54	1.795	0.125	0.946	0.0661	12.425	0.868
Phenanthrene	4.57	1.969	0.128	1.038	0.0673	13.630	0.883
Pyrene	5.17	12.539	0.181	6.611	0.0957	86.796	1.256
Fluoranthene	5.22	14.630	0.187	7.714	0.0985	101.274	1.294
Benzo[a]anthrecene	5.84	99.097	0.269	52.246	0.142	685.96	1.862
Chrysene	5.84	99.097	0.269	52.246	0.142	685.96	1.862
Benzo [a]pyrene	6.04	183.679	0.302	96.840	0.159	1271.446	2.094
Benzo[b]fluoranthene	6.44	480.240	0.363	253.194	0.191	3324.282	2.511
Benzo[k]fluoranthene	6.44	480.240	0.363	253.194	0.191	3324.282	2.511
Indeno[1,2,3-cd]pyrene	6.58	480.240	0.325	253.194	0.171	3324.282	2.248
Benzo[ghi]perylene	6.90	480.240	0.252	253.194	0.133	3324.282	1.746

3.2.2. Bioaccumulation in zooplankton

In the case of zooplankton, we have also to consider the intake due to food consumption as well as the egestion and metabolization (Berrojalbiz et al., 2006). In this case the concentration of a chemical in the two zooplankton groups (C_{Zs} ,C_{Zl}) over time can be expressed as:

$$\frac{dC_{Zs}}{dt} = k_u^{Zs} \cdot C_{PAH}^{dis} + k_g^{Zs} \cdot C_p - k_d^{Zs} \cdot C_{Zs} - k_e^{Zs} \cdot C_{Zs} - k_m^{Zs} \cdot C_{Zs} \tag{42}$$

$$\frac{dC_{Zl}}{dt} = k_u^{Zl} \cdot C_{PAH}^{dis} + k_g^{Zl} \cdot C_p - k_d^{Zl} \cdot C_{Zl} - k_e^{Zl} \cdot C_{Zl} - k_m^{Zl} \cdot C_{Zl} \tag{43}$$

where k_g ($m^3 \cdot kg^{-1} \cdot d^{-1}$) , k_e (d^{-1}) and k_m (d^{-1}) are the grazing, egestion and metabolization rate constants. These constants have been obtained experimentally by Berrojalbiz et al. (2006) for several PAHs. In Table 3.2 we report the values found for the PAHs taken into consideration by the model developed.

Table 3.2. Uptake ($m^3 \cdot kg^{-1} \cdot d^{-1}$), depuration ($d^{-1}$),grazing ($m^3 \cdot kg^{-1} \cdot d^{-1}$), egestion ($d^{-1}$) and metabolism ($d^{-1}$) constants used in the model (Berrojalbiz et al., 2006).

Compound (PAHs)	k_u^Z	k_d^Z	k_g^Z	k_e^Z	k_m^Z
Fluorene	1.23	69.38	1.21	9.95	0.56
Phenanthrene	23.04	167.56	5.41	10.37	0.39
Pyrene	113.27	371.78	128.06	17.86	1.03
Fluoranthene	117.230	519.87	115.87	19.64	0.99

3.3. INTRODUCTION OF TOXIC EFFECTS

Mortality of the different components of the trophic food chain has been modeled based on dose-response data for phytoplankton from Grote *et al.* (2005), Djomo *et al.* (2004) and Bopp and Lettieri (2007), and from zooplankton from http://www.pesticideinfo.org/. No data has been found for bacteria, therefore the toxicity data have been assumed low and comparable with unicellular species in the above mentioned database. In this model the dose-response effects have been simulated using the Weibull equation:

$$f(x) = 1 - \exp[-\exp(\theta_1 + \theta_2 \log_{10} x)] \qquad (44)$$

Table 3.3 shows the fitted parameters concerning Pyrene, whereas fig. 3.2 shows the calculated curves for phytoplankton, zooplankton and bacteria.

Table 3.3. Parameters for the Pyrene dose-response function in the model.

Parameter	**Phytoplankton, flagellates[1]**	**Phytoplankton, diatoms[2]**	**Zooplankton (both types)[3]**	**Bacteria[4]**
θ_1	-9.072	3.041	-10.442	-15.8486
θ_2	5.143	1.142	5.143	5.143

[1]from Grote *et al.* (2005);[2]from http://www.pesticideinfo.org/ (Daphnia Magna, EC_{50} 91.02 µg/L); [4]No data found

In the model, the mortality of the ecological compartments is changed as a function of the concentration of contaminant by adding to the mortality rate in the original equations, Eqs. (1)-(5), the induced pyrene mortality as given by Eq. (44). In addition this mortality term produces an increase in the detritus fraction and therefore a change in the distribution of the contaminant between dissolved and particulate phases.

Since Pyrene is the only PAHs that has been tested in mesocosm experiments and the environmental concentrations are quite low, we will validate these expressions when this model will be validated using mesocosm data sets provided by NERI when studying the combined effects of nutrients and contaminants.

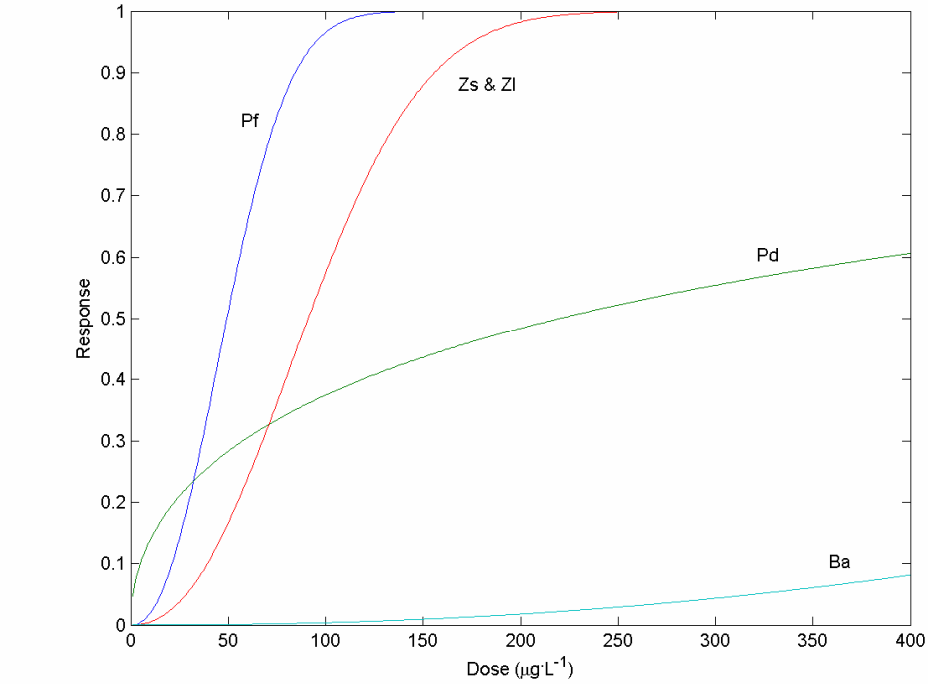

Figure 3.2. Dose-response curves for phytoplankton (Pf and Pd), zooplankton (Zs and Zl) and bacteria (Ba) for pyrene.

4. Introducing ecosystem dynamics and bioaccumulation in a 1D hydrodynamic-contaminant fate model

The 1D (vertical) hydrodynamic-contaminant fate model has already been described extensively in D2.6.2 where the model structure, functioning, processes (partitioning, atmospheric exchange, settling, degradation, resuspension, burial and diffuse interaction with sediments) as well as the simulation results were presented for selected POPs families: PCBs, PAHs, PBDEs and PCDD/Fs. However, we were not able to find experimental data sets to validate the model results and there was no direct link with the coastal/marine ecosystems as well as with the relationships between contaminant concentrations in the water and those in the biological compartments. Therefore, in this report we are going to focus on the coupling of the previously developed 1D hydrodynamic-contaminant fate model with the ecological food-web and bioaccumulation models described above. The final objective is to develop a comprehensive integrated model for assessing the effects of POPs in the aquatic environment at ecosystem level. In addition, the work aims to perform extended testing, verification and assessment of contaminant fate model against observations, in particular for PAHs, since in Thresholds project natural communities (ref.) as well as mesocosm experiments were carried out using PAHs mixtures and Pyrene (Dahllöf and Hjorth, 2006), respectively. So far, studies on the role of zooplankton metabolism in marine ecosystems has been also developed using PAHs mixtures (Berrojalbiz et al., 2006). Technically the coupling is achieved by an incorporating of last two modules (food-web and bioaccumulatgion) into the program structure of 3D COHERENS model (Luyten *et al*., 1999) keeping hydrodynamic/physical part unchanged and using numerical solvers of the original model code for newly added contaminant, ecological and bioaccumulation compartments.

In order to assess the performance of any aquatic contaminant fate model, the availability of detailed spatial and timely synchronized measurements in all environmental compartments (atmosphere, water column, sediments, and ecosystem) is essential. Unfortunately, such kind of data sets, in particular for Mediterranean region, is difficult to find. This was one of the reasons for two Mediterranean cruises organized during the Thresholds Project during 2006 and 2007 (experimental data are being processed by the laboratory partners participants). In the mean time, some recent studies about PAHs (Tsapakis et al., 2005 and Tsapakis et al., 2006) and PCBs (Schultz-Bull et al.,1997; Mandalakis and Stephanou, 2004 and Mandalakis et al., 2005) in Eastern Mediterranean have been also published. In these publications detail information about atmospheric gas and particulate phases, rain water concentrations, dry and wet deposition, air-sea exchange, dissolved seawater concentrations and sediment trap fluxes

collected during a two-year period (November 2000 – July 2002) off-shore near to Finokalia station (35°19' N, 25°40' E, Island of Crete, Greece) are presented. Then, these data have been identified as enough complete to feed the model with necessary forcing, initial and boundary information and on the other hand sufficient to verify simulation results against the measured seawater concentrations and air-water fluxes.

4.1. MODEL FORCING DATA SETS

The present integrated contaminant fate model for the open sea environment has been tested at Finokalia observation station in Eastern Mediterranean (35°19' N, 25°40' E, Island of Crete, Greece), location with an average depth of 200m, supposed to be a remote site faraway from anthropogenic influences. At these conditions the internal water mixing is expected to be mainly generated by atmospheric forcing at the air-sea interface, while the tidal action to be almost unimportant. The model spatial resolution is 200 vertical layers (1m per layer) and the time step, restricted by the barotropic mode, is fixed to 60s. The meteorological forcing in use is obtained from six-hour measures provided by the European Center for Medium Weather Forecast (ECMWF, http://www.ecmwf.int), namely: air temperature at 2m, wind speed and direction at 10m, precipitation rate, cloud cover, and relative humidity, which were referred to the two-year time period of 2001-2002 at the buoy location (see Fig. 4.1). A linear interpolation has been employed to recalculate the forcing functions with hourly frequency. Besides, the hydrodynamic part was initialized with constant vertical profiles for temperature (T=13.5° C) and salinity (S=38.5 ‰). Similar approach has been used for initialization of all other ecological and chemical compartments being part of the integrated model. The model has been run for two-year time period ongoing from 1st of January 2001.

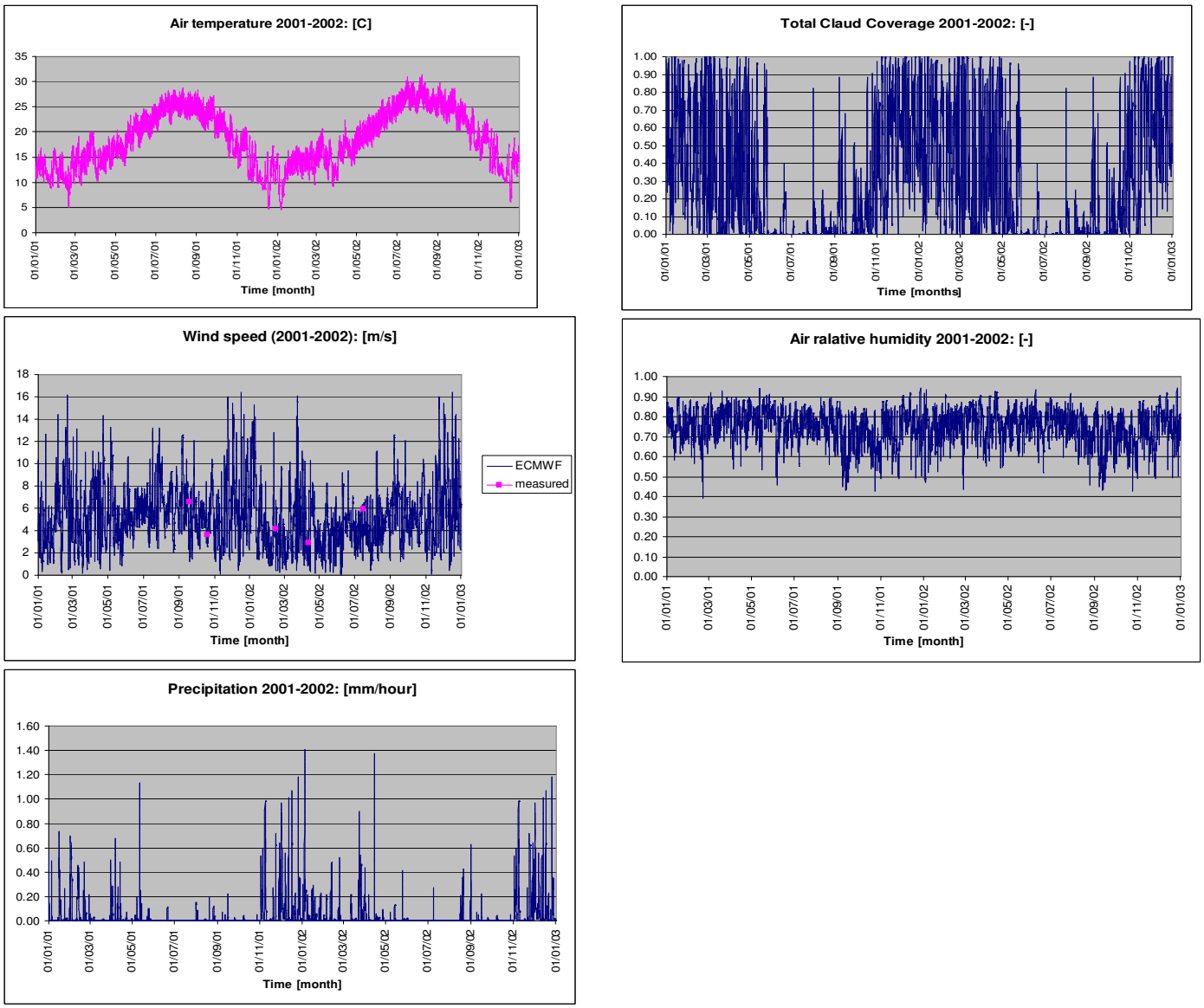

Fig. 4.1. Meteorological forcing obtained from six-hour measures provided by the European Center for Medium Weather Forecast (ECMWF, http://www.ecmwf.int): air temperature at 2m, wind speed and direction at 10m, precipitation rate, cloud cover, and relative humidity, referred to two-year time period of 2001-2002 at Finokalia observation station, Eastern Mediterranean (35°19' N, 25°40' E, Crete, Greece). A linear interpolation has been employed to recalculate the forcing functions with hourly frequency.

4.2. MODEL VALIDATION: TEMPERATURE AND SALINITY

The first step in the validation of the model is to compare the temperature and salinity measurements with model output for Finokalia station using the forcing conditions obtained from ECMWF. Figure 4.2 shows the numerical results about surface salinity and temperature, compared with monthly average data taken from the Environmental Marine Information System (EMIS, http://emis.jrc.ec.europa.eu), a reliable mixture of satellite observations and simulations. In general, the simulated temperature values

and seasonality variations are predicted by the model with lower than 10% error levels while for salinity the fluctuations are in the 1% range.

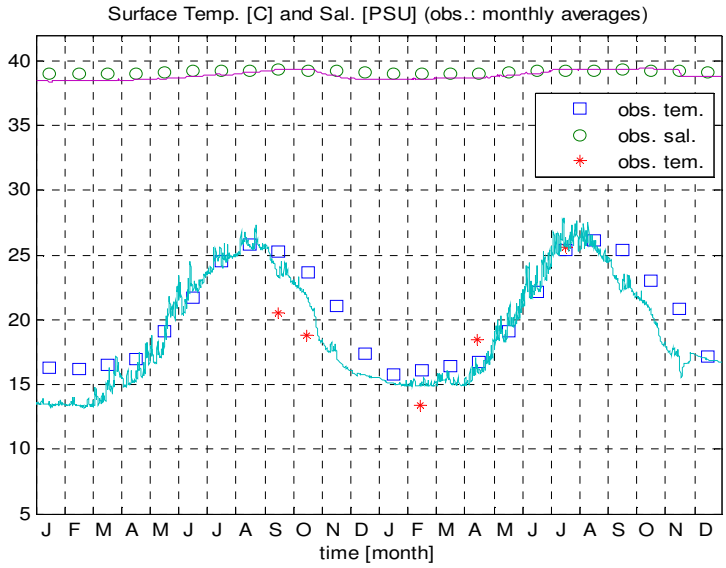

Figure 4.2. Comparison of observed and simulated temperatures (°C) and salinity (‰) at Finokalia station. Experimental data are taken from the Environmental Marine Information System (EMIS, http://emis.jrc.ec.europa.eu) of JRC and from Tsapakis et al. (2006).

4.3. MODEL VALIDATION: PAHs DYNAMICS IN THE WATER COLUMN

Based on the detailed input/forcing information, provided by Tsapakis et al. (2005) and (2006), the model has been tested and validated for seven PAHs, namely: fluorene, antracene, phenanthrene, pyrene, fluoranthene, benzo[a]anthracene and chrysene. The main differences of this model results in comparison with the results given in Deliverable 2.6.2, consists in the forcing data and the use of a different formula for temperature dependence of Henry's law - the generalized formula of Paasivirta et al. (1999), derived for 73 persistent organic pollutants, including polychlorinated biphenyls, diphenylethers, dibenzo-*p*-dioxins, and dibenzofurans, organochlorinated pesticides and polycyclic aromatic hydrocarbons, has been replaced by a relation of Nelson et al. (1998), specifically constructed for PAHs and PCBs using Chesapeake Bay observations. This correlation has improved considerable the comparison between experimental and simulated results. A detail investigation on the impact of Henry's law relations is foreseen for our future work.

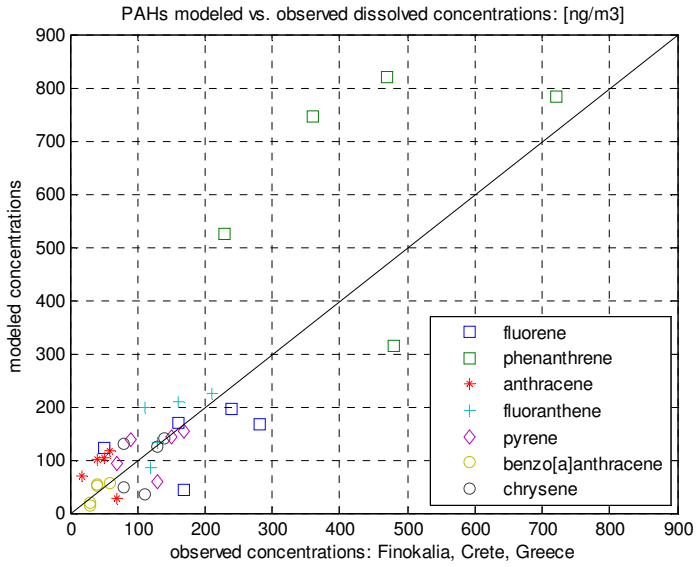

(a)

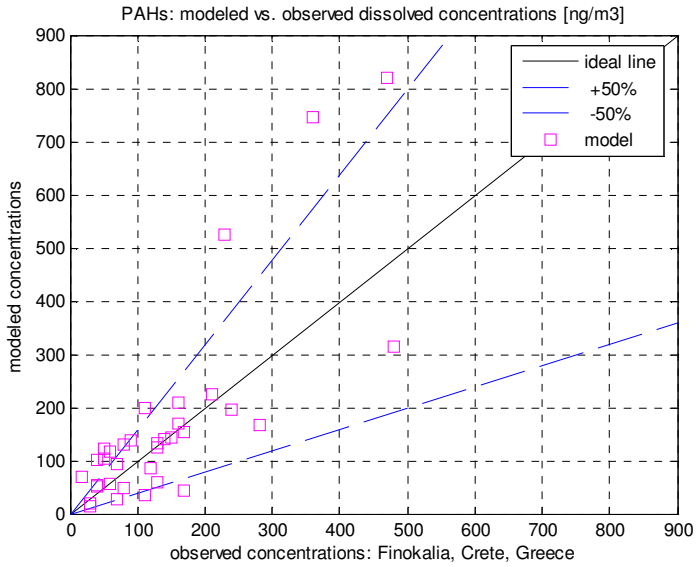

(b)

Figure 4.3. a/ Comparison between experimental and simulated concentrations for all seven PAHs considered (fluorene, antracene, phenanthrene, pyrene, fluoranthene, benzo[a]anthracene and chrysene) R^2=0.72; b/ ±50% error zone around ideal lines (experimental data from Tsapakis et al., 2006).

A general comparison between experimental and simulated dissolved concentrations for all seven PAHs considered (fluorene, antracene, phenanthrene, pyrene, fluoranthene, benzo[a]anthracene and chrysene) is shown in Figure 4.3 for the surface layer of the water column. As can be seen, there is a good agreement (R^2=0.72) between experimental and simulated results practically for all PAHs. This conclusion is confirmed again by designing ±50% error zone around the ideal line when it was found

that mostly of numerical predictions not exceed or are of order of 50% deviation compared to measurements.

In addition, the Figure 4.4 shows the detailed comparison between experimental and the two years simulated concentrations in dissolved phases for the surface layer of the water column. In order to complete the picture of environmental fate of PAHs the total, particulate and DOC phase concentrations are also presented on the same figures. As can be see the lighter PAHs are more associated to the dissolved phase whereas the partitioning to the particulate phase increases as the octanol-water partition coefficient increases.

However, in spite of the common good agreement between experimental and simulated results, the reduced number of experimental points available does not allow providing general assessment or conclusions on the ability of the model to capture the entire PAHs dynamics. The model predicts well a seasonal cycle (see Fig. 4.4), following the water temperature variations and vertical water column stratification, with typical low concentrations during the late autumn and winter and higher concentrations in the water column during late spring, summer and early autumn, when the vertical mixing is termocline blocked. More experimental observations would be necessary to validate this aspect.

Figure 4.5 shows for the specific case of pyrene the simulated results in terms of total concentration over the two year period as well as the particulate phase concentrations over the same period. In both cases the seasonal variation can be clearly observed.

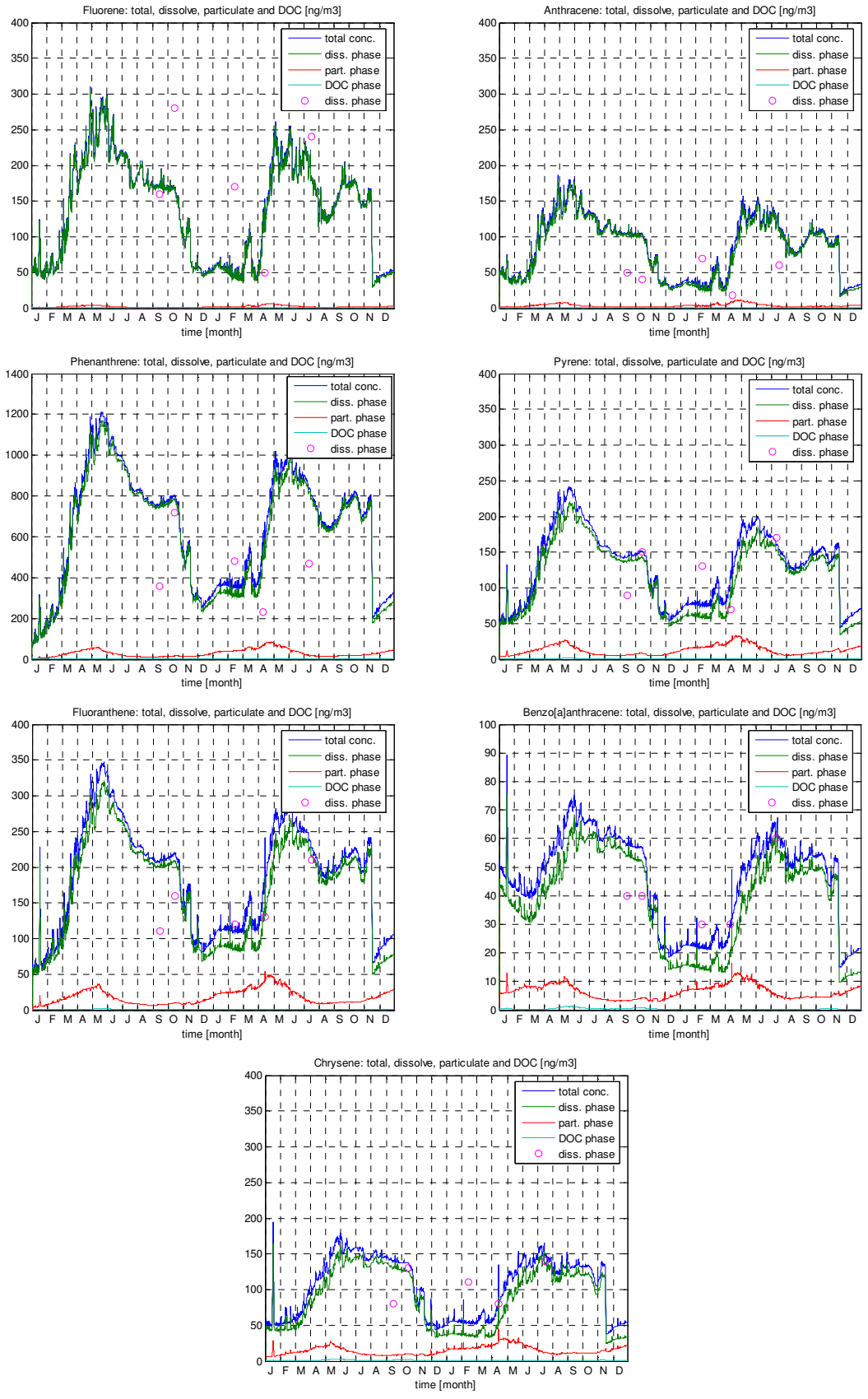

Figure 4.4. Comparison between experimental (dissolved phase) and two-years simulated (dissolved, particulate and attached to DOC) concentrations for all seven PAHs considered (experimental data from Tsapakis et al., 2006).

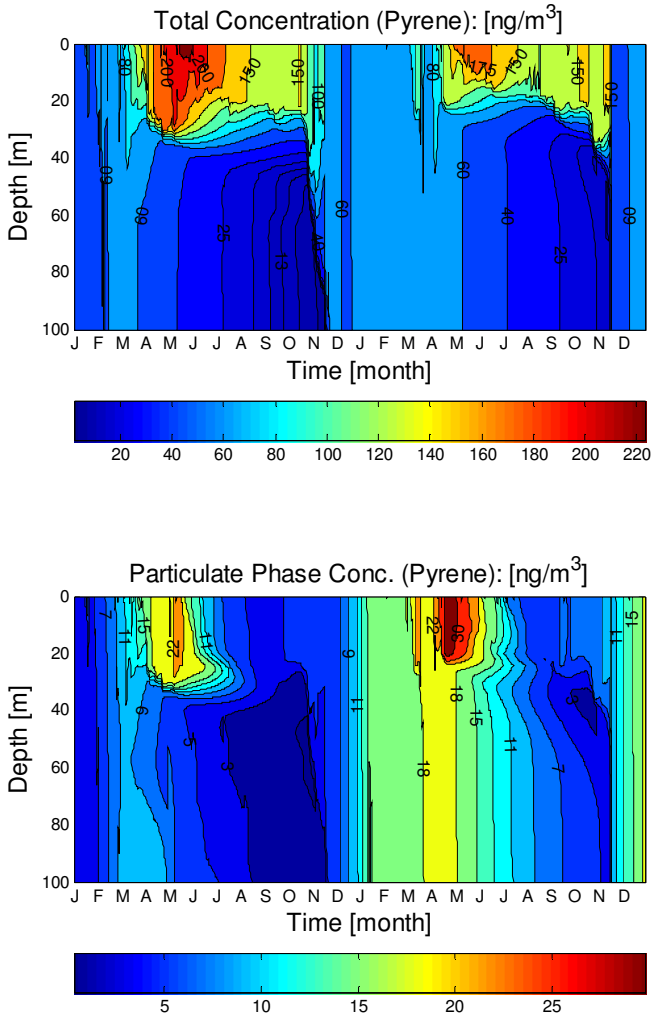

Figure 4.5. Annual dynamics of PAHs (Pyrene) in a vertical profile (top hundred meters) of the water column given in (a)-total and (b)-particulate concentrations during two-years period.

4.4. MODEL VALIDATION: PAHs FLUXES

A further validation of the model performance has been done by comparing experimental and simulated air-water fluxes. Table 4.1 summarizes the results obtained. As it can be seen, with the exception of fluorene (it demonstrates maximum deviation of 199% as a lighter one, while minimum of 22.6% is found for the heavies studied PAH compound), the values obtained are in a close agreement with the field measurements (Tsapakis et al., 2006). Then, the estimated average deviation for AW flux of PAHs (seven congeners) is about 62.95% (only 40.28% if Fluorene is excluded).

Table 4.1. Comparison between experimental and simulated annual air-water fluxes for PAHs (experimental data from Tsapakis et al., 2006).

	Atmosphere Concentrations			**Total Air-Water Flux [µg/m2/year]**	
	Gas [ng/m3]	**Particulate [ng/m3]**	**Rain [ng/L]**	**Observed**	**Modeled**
Fluorene	1.040	0.02	3.2	21.4	64.1 (+199%)
Anthracene	0.614	0.004	8.1	32.5	43.3 (+33.2%)
Phenanthrene	4.784	0.05	61.2	336.1	180.4 (-46.3%)
Pyrene	0.650	0.04	17.2	68.4	39.1 (-42.8%)
Fluoranthene	0.818	0.10	59.6	87.3	52.6 (-39.7%)
Benzo[a]anthracene	0.068	0.03	8.2	3.5	5.6 (+57.1%)
Chrysene	0.176	0.10	46.9	21.2	17.1 (-22.6%)

Average deviation for AW flux: 62.95%; 40.28% excluding Fluorene

Additionally, in order to discuss the air-water fluxes dynamics, we have plotted in Fig. 4.6a the results of the dynamics on wet, dry and air-water gas exchange (referred as *AW gas*) as well as the corresponding experimental results of Tsapakis et al., 2006. Moreover, the Fig. 4.6b shows the specific atmospheric-ocean gas exchange in terms of absorption (marked as *abs*) and volatilization (marked as *vol*) fluxes that compose the dominant part of the air-water mass transfer. It was found that the deposition fluxes are higher during the winter due to temperature influence on air-water partitioning and water particle partitioning. Furthermore, the high biomass during phytoplankton blooms, occurring in early spring and autumn may produce an enhanced net air-water diffusive exchange. As confirmed in other studies (Jurado et al. 2004), the diffusive fluxes dominate the total atmospheric deposition flux.

Finally, Figure 4.7 shows the annual integrated fluxes (daily average for a period of one year and total annual). The total flux predicted here is within a factor of two of that reported in the field experiments. However, this error is reasonable due to the uncertainties (errors) in predicted concentrations and different parameterizations between simulations and field measurements. Furthermore, the approach used here has the advantage of providing values for the seasonality of the fluxes and of allowing to study the influence of planktonic food web on these values.

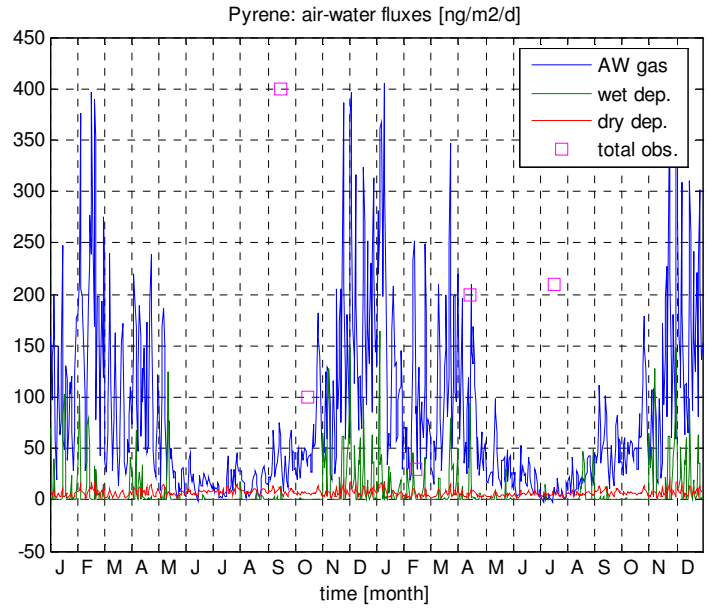

a/

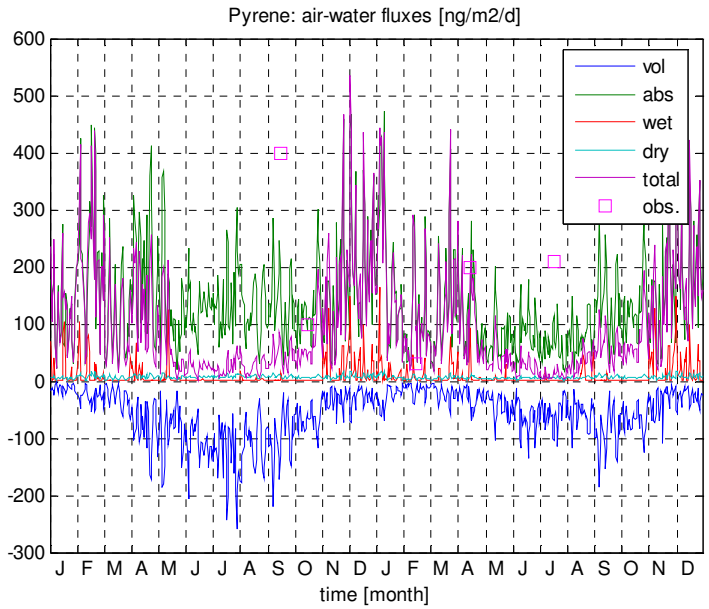

b/

Figure 4.6. Simulated and experimental daily air-water fluxes (wet, dry and air-water gas exchange - referred as *AW gas,* absorption (*abs*) and volatilization (*vol*)) for Pyrene. Experimental data from Tsapakis et al., (2006).

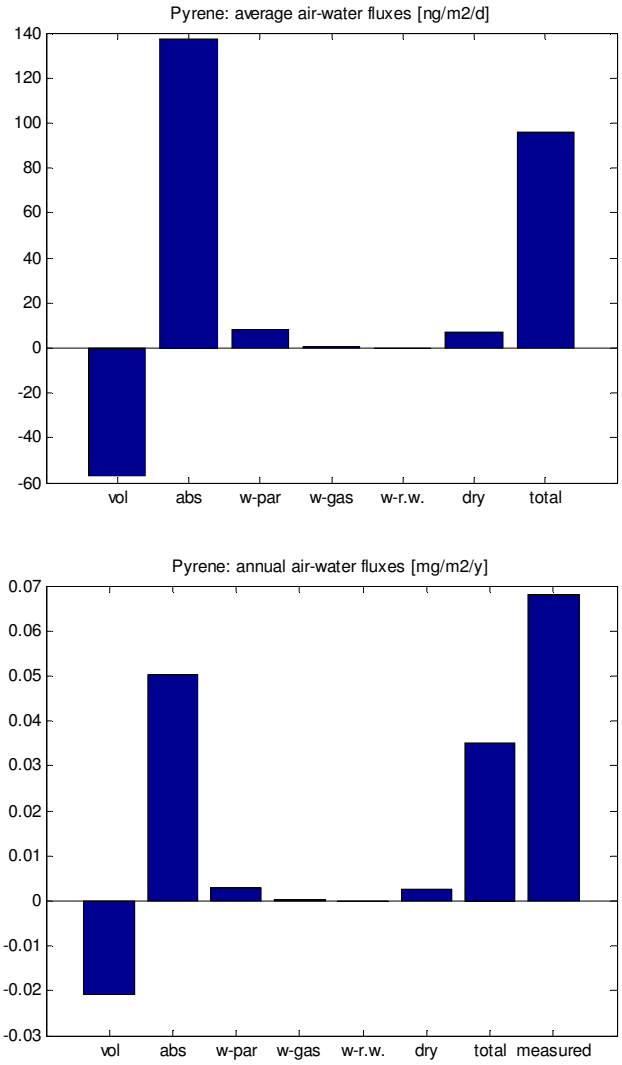

Figure 4.7. Simulated and experimental daily annually average and total annual air-water fluxes (absorption - marked as (*abs*), volatilization (*vol*), wet-particulate, wet-gas, wet-rain water and dry) for Pyrene. Experimental data from Tsapakis et al., (2006).

4.5. BIOLOGY: SIMULATED RESULTS

Before starting with the verification of the results of the ecological part of the model, it worst to explain how the coupling between biology and contaminant fate models was performed. The biological sub-model allows calculating the spatial-temporal Particulate Organic Carbon distribution in the water column by suggesting *POC* = *Detritus* + *Bacteria* + *Phytoplankton* + *Zooplankton* (mg C.m^{-3}). Then, turning to the contaminate fate model we assumed that the Particulate Organic Matter is *POM=2*POC* following Hedges et al. (2002) as well as the Dissolved Organic Carbon is correlated with POC according to Vallino (2000). Furthermore, the zooplankton metabolism is also included in the fate model as an additional decomposition rate term (last terms in the Eqs.42-43).

For assessment of the results produced by the ecosystem model, we have been able to find Chlorophyll a data at the Environmental Marine Information System (EMIS, http://emis.jrc.ec.europa.eu), for the simulated periods. The comparison between experimental (monthly averages) and simulated values is shown in Figure 4.8. Information for other trophic levels/compartments of the ecosystem (micro and meso zooplankton, bacteria and detritus) is presented additionally in Figure 4.9.

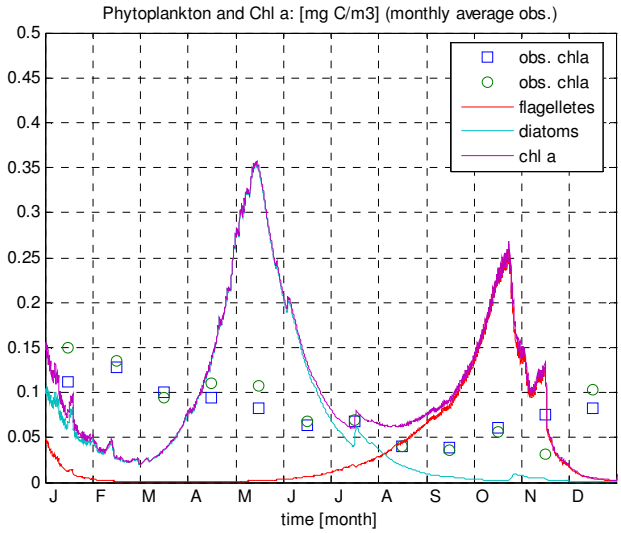

Figure 4.8. Comparison of simulated and observed chl-a concentrations for one–year period. The monthly average experimental data are taken from the Environmental Marine Information System (EMIS, http://emis.jrc.ec.europa.eu) of JRC.

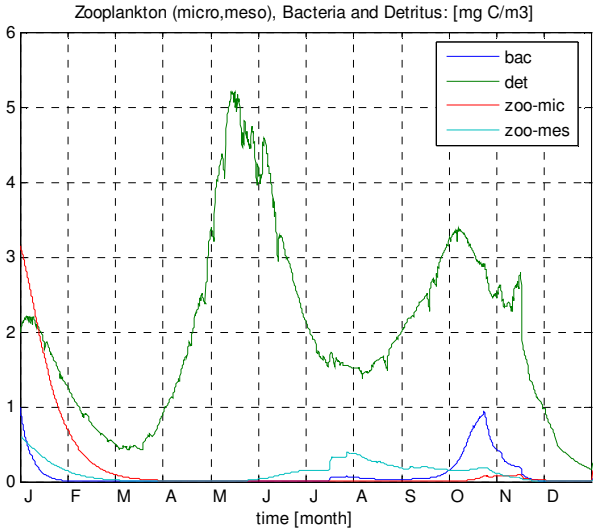

Figure 4.9. Simulated low trophic levels/compartments of the ecosystem (micro and meso zooplankton, bacteria and detritus) for one–year period.

Similarly to the contaminant module testing, also a good agreement in terms of chlorophyll a magnitude and its seasonal dynamics was found. However, the peaks of chlorophyll a (phytoplankton blooms) are not correctly simulated, but this issue is usually difficult to address (Zaldivar et al., 2003). Actually, the fact that chlorophyll a is in a proper order of magnitude is more important for the validation of the integrated contaminant fate model, since POPs dynamics depend strongly not only on

temperature (air-water exchange), but also on organic matter and particles - inorganic TSM is also calculated by the model (see D2.6.2 and Jurado et al. 2007), available into the system (partitioning between dissolved and particulate concentrations) which amount is provided by the ecological model simulations.

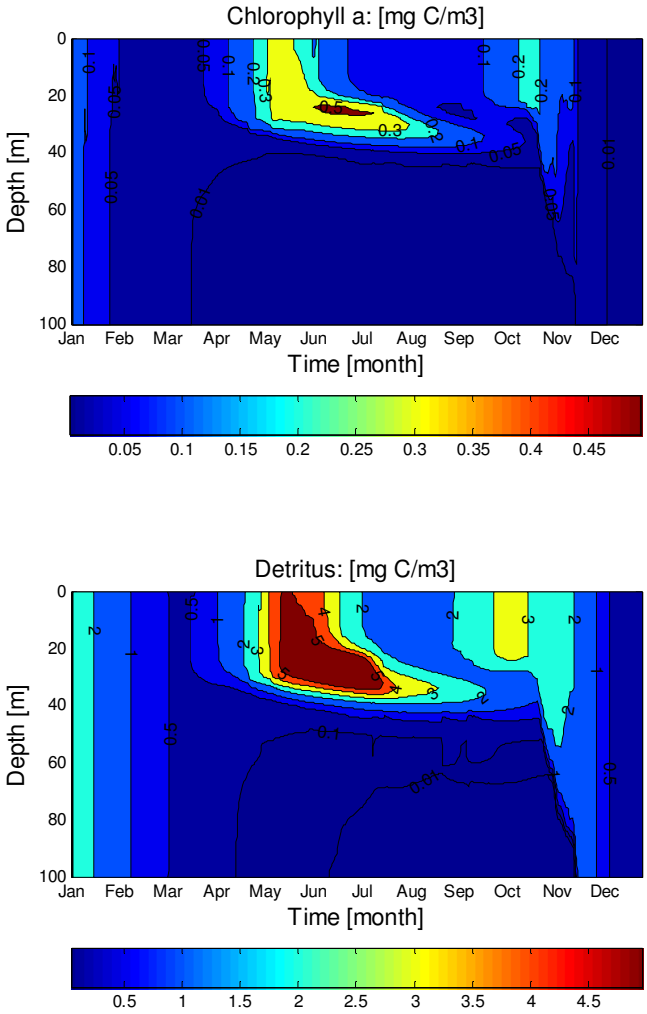

Figure 4.10. Annual dynamics of Chlorophyll a and Detritus in a vertical profile (top hundred meters) of the water column during one-year period.

In addition, to complete the spatial-temporal presentation of primary production and lower trophic levels of the ecosystem, the annual dynamics of Chlorophyll a and Detritus (the other compartments have quite similar behavior) in a vertical profile (top hundred meters) of the water column during a period of one-year cycle, are provided in Figure 4.10. Here it is interesting to mention that the model reproduce correctly the typical annual cycle (spring and early autumn blooms of primary production) and the effect of 'diving' (following the better living conditions) in the summer time of the year which is also observed in other field measurements.

4.6. SIMULATED CONCENTRATIONS IN BIOTIC COMPARTMENTS

As stated before the present integrated model is foreseen not only for calculating the pollutants distribution/fate in the water column, but also the bioaccumulation and biomagnification of POPs into different biotic compartments, starting with the primary producers (phytoplankton) and continuing with higher trophic levels. For that reason we have been able to simulate the PAHs concentrations in several biota compartments for four selected congeners (fluorene, phenanthrene, pyrene and fluoranthene), for which experimentally estimated uptake, depuration, grazing, egestion and metabolization rate constants for zooplankton were available (Berrojalbiz et al., 2006).

In general, the PAHs concentrations in phytoplankton - see Figure 4.11a – follow the dynamics of the dissolved concentrations in the water column (see Fig.4.4) and ecosystem seasonal/annual cycling (see Fig.4.8). This fact explains the lower PAHs concentrations found in the phytoplankton compartment during the winter period, which growth in the spring (dissolved concentrations are growing and phytoplankton is blooming) and reach their annual maximum (May-June), then gradually decline in the summer followed by a little autumn increase (the second phytoplankton bloom) and finally in late autumn they fall to the usual winter values. Furthermore, the simulations evidence that the lighter PAHs are considerably less concentrated, with almost constant contaminant concentrations during the entire year.

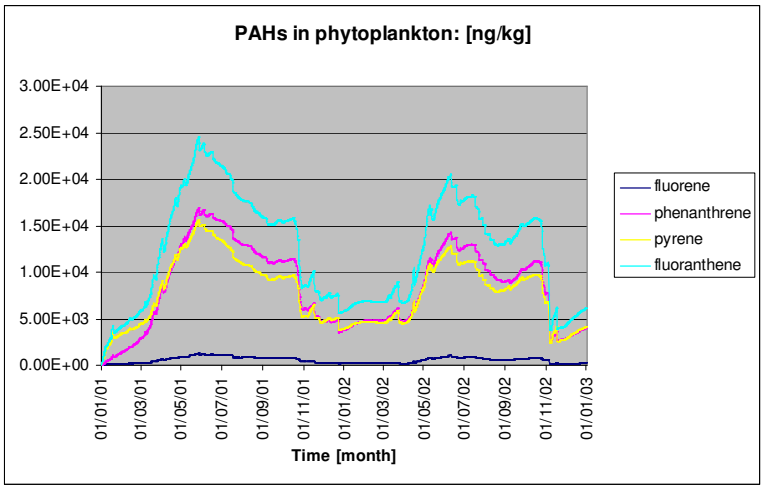

a/

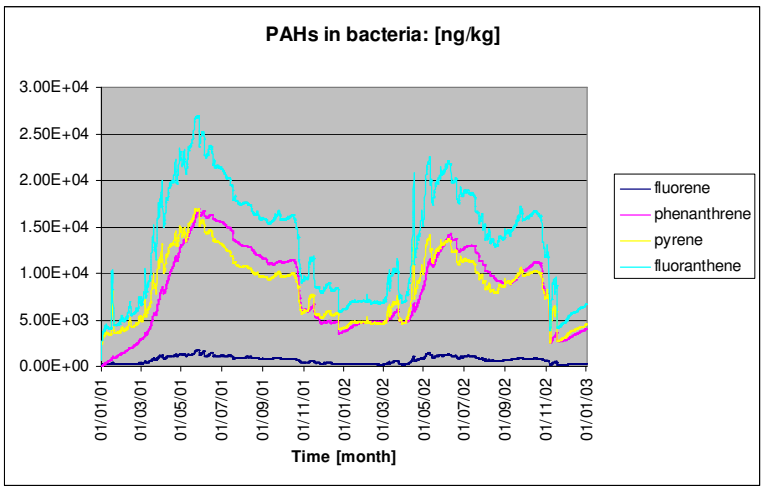

b/

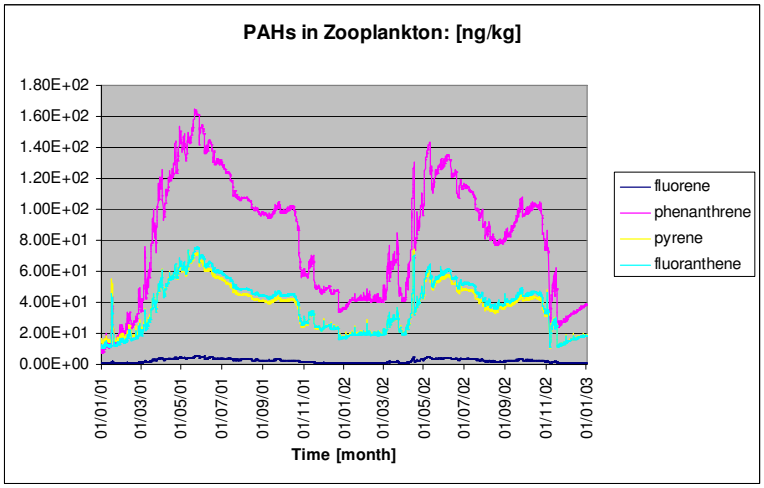

c/

Figure 4.11. Simulated PAHs concentrations (fluorene, phenanthrene, pyrene and fluoranthene) in biotic compartments: a/ phytoplankton; b/ bacteria; c/ zooplankton, during two-years period.

The other biotic compartments (bacteria and zooplankton) demonstrate similar annual/seasonal dynamics (see Fig. 4.11b-c) but with higher daily oscillations. Moreover, since its specific metabolic/depuration processes the zooplankton actually has very little PAHs concentrations as it can be seen in Fig. 4.11c. In this case the PAHs concentrations are more than two order of magnitude lower when compared with the concentrations in the other trophic compartments. It is also interesting to mention that during the two Mediterranean Thresholds cruises, the estimated summer PAHs concentrations in a planktonic net (size of 100µm) were as follows: fluorene – 60ng/g; phenanthene – 200ng/g; pyrene – 100ng/g; and fluoranthene – 100ng/g (these are the values for the light part of the day, the nocturnal ones are usually 2-2.5 times smaller), while for example the model predicts an annual average pyrene concentration about 7.8ng/g for a single groups of flagellates or diatoms (similar value for bacteria).

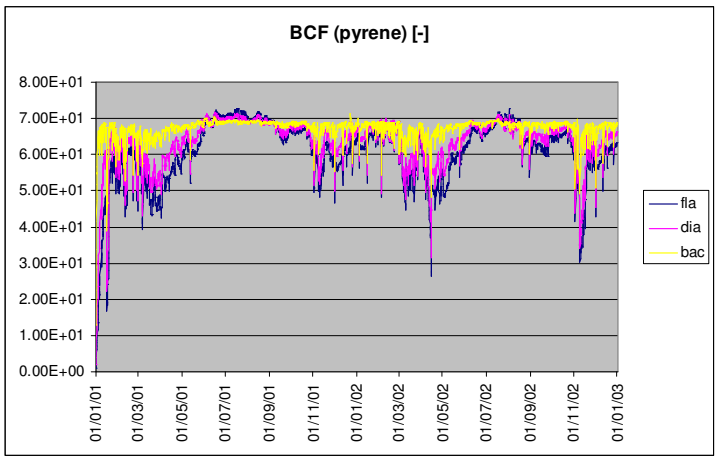

a/

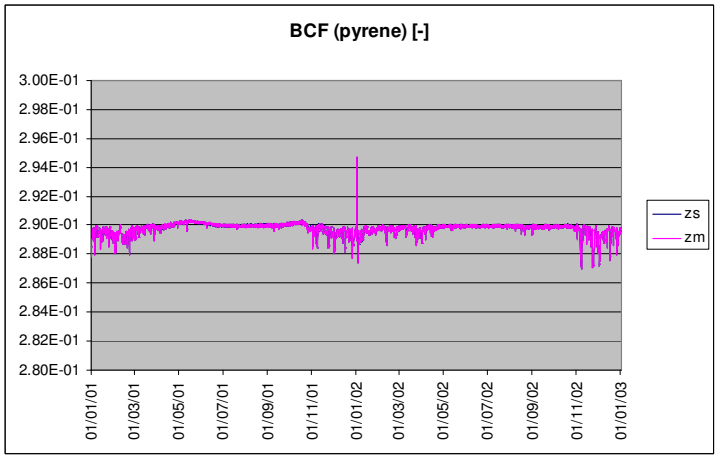

b/

Figure 4.12. Simulated bioconcentration factor of pyrene in different biotic compartments: a) phytoplankton and bacteria; b) micro and meso-zooplankton, during two-years period.

Finally, using the model we have calculated the Bioconcentration Factor (BCF) for PAHs. In Figure 4.12, as an example, the BCF is given for Pyrene during two-years period. For phytoplankton group the BCF is seasonably variable with typical winter values of 4.5-5.5 and maximum summer ones of order 7, respectively. The zooplankton species keep almost constant BCF during the year equals to 0.289 – a number quite bellow one, which follows the experimental results from Berrojalbiz et al. (2006) concerning the zooplankton metabolization. In this sense, this indicates that bioaccumulation through the food chain would be reduced concerning PAHs when compared with other POPs such as PCBs, PCFF/Ds or PBDEs.

5. Conclusions

In this report, an integrated model, including fate of contaminants and ecological models, is presented. The model has been developed in the framework of the Thresholds project for analysing the effects of contaminants at ecosystem level. The model allows estimating the environmental concentrations of POPs and the main fluxes between compartments, i.e. air/water/sediments and organisms. In addition the model has been validated for PAHs based on experimental data available in literature. It is expected that, when experimental data will be available, the model will be also verified for other POPs families such as PCBs, PBDEs and PCCD/Fs.

However, even though the model is able to predict environmental concentrations and fluxes between compartments with good accuracy, the validation of the observed dynamics would require far more datasets that those available in literature.

6. References

Altenburger, R; Walter, H and Grote, M. 2004. What Contributes to the Combined Effect of a Complex Mixture? *Environ. Sci. Technol*. **38**, 6353-6362.

Baker, J.E., Eisenreich, S.J., Eadie, B.J., 1991. Sediment trap fluxes and benthic recycling of organic carbon, polycyclic aromatic hydrocarbons, and polychlorobiphenyl congeners in Lake Superior. *Environ. Sci. Technol*. **25**, 500–509.

Berglund, O., Larsson, P., Ewald, G., Okla, L., 2001. Influence of trophic status on PCB distribution in lake sediments and biota. *Environmental Pollution* **113**, 199–210.

Berrojalbiz, N., Lacorte, S., Barata, C., Calbet, A. and Dachs, J. 2006. Accumulation of low MW polycyclic aromatic hydrocarbons in marine phytoplankton, zooplankton and fecal pellets. Thresholds IP, Stream 4 Meeting, 2nd-3rd May, Barcelona.

Boese, B. 1984. Uptake efficiency of the gills of English sole (Parophrys vetulus) for four phthalate esters. *Can. J. Fish. Aquat. Sci.* **41**, 1713-1718.

Bogdan, J.J., Budd, J.W., Eadie, B.J., Hornbuckle, K.C., 2002. The effect of a large resuspension event in southern Lake Michigan on the short term cycling of organic contaminants. *Journal of Great Lakes Research* **28**, 338–351.

Boop, S. and Lettieri, T., 2007. Gene Regulation in the Marine Diatom *Thalassiosira pseudonana* upon Exposure to Polycyclic Aromatic Hydrocarbons (PAHs) *Gene* **396**, 293-302.

Carafa, R., Marinov, D., Dueri, S., Wollgast, J., Ligthart, J., Canuti, E., Viaroli, P. and Zaldívar, J. M., 2006. A 3D hydrodynamic fate and transport model for herbicides in Sacca di Goro coastal lagoon (Northern Adriatic). *Mar. Poll. Bull*. **52**, 1231-1248.

Dachs, J., Bayona, J.M., Albaiges, J., 1997. Spatial distribution, vertical profiles and budget of organochlorine compounds in Western Mediterranean seawater. Marine Chemistry 57 (3–4), 313–324.

Dachs J., Lohmann, R., Ockenden, W. A., Eisenreich, S.J. and Jones, K. C., 2002, Oceanic Biogeochemical Controls on Global Dynamics of Persistent Organic Pollutants.*Environ. Sci. Technol*. **36**, 4229-4237.

Dachs, J., Eisenreich, S., Baker, J. E., Ko, F.-C. and Jeremiason, J. D., 1999. Coupling of phytoplankton uptake and air-water exchange of persistent organic pollutants. *Environ. Sci. Technol*. **33**, 3653-3660.

Dahllöf, I. and Hjorth, M. 2006. Effect of pyrene on plankton communities: modelling of direct and indirect effects. Thresholds IP, Stream 4 Meeting, 2nd-3rd May, Barcelona.

Dalla Valle, M., Marcomini, A., Sfriso, A., Sweetman, A.J., Jones, K.C.,2003. Estimation of PCDD/F distribution and fluxes in the Venice Lagoon, Italy: combining measurement and modelling approaches.*Chemosphere* **51**, 603–616.

Del Vento, S. and Dachs, J., 2002. Prediction of uptake dynamics of persistent organic pollutants by bacteria and phytoplankton. *Environmental Toxicology and Chemistry* **21**, 2099-2107.

Devillers, J., Bintein, S., Domine, D., 1996. Comparison of BCF models based on log P. *Chemosphere* **33**, 1047-1065.

Djomo, JE; Dauta, A; Ferrier, V; Narbonne, JF; Monkiedje, A; Njine, T and Garrigues, P., 2004. Toxic effects of some major polyaromatic hydrocarbons found in crude oil and aquatic sediments on *Scenedesmus subspicatus*. *Water Research* **38**, 1817-1821.

Hailiang, D., Rothmel, R., Onstott, T.C., Fuller, M.E., DeFlaun, M. F., Streger S. H., Dunlap, R., and Fletcher, M., 2002. Simultaneous Transport of Two Bacterial Strains in Intact Cores from Oyster, Virginia: Biological Effects and Numerical Modeling. *Applied and Environmental Microbiology* **68**, 2120-2132.

Dueri, S., Zaldívar, J.M. and Olivilla, A., 2005. Dynamic modelling of the fate of DDT in lake Maggiore: Preliminary results. EUR report n° 21663. JRC, EC. pp. 33.

Fisk, A.T., Norstrom, R.J., Cymbalisty, C.D., Muir, D.C.G., 1998. Dietary accumulation and depuration of hydrophobic organochlorines: bioaccumulation parameters and their relationship with the octanol/water partition coefficient. *Environ. Toxicol. Chem*. **17**, 951-961.

Gobas, F.A.P.C., Muir, D.C.G., Mackay, D., 1988. Dynamics of dietary bioaccumulation and feacal elimination of hydrophobic organic chemicals in fish. *Chemosphere* **17**, 943-962.

Gobas, F.A.P.C., Wilcockson, J.B., Russell, R.W., Haffner, G.D., 1999. Mechanism of biomagnification in fish under laboratory and field conditions. *Environ. Sci. Technol*. **33**, 133-141.

Grote, M; Schuurmann, G and Altenburger, R. 2005. Modeling photoinduced algal toxicity of polycyclic aromatic hydrocarbons. *Environ. Sci. Technol.*39, 4141-4149.

Gunnarsson, J. S. and Sköld, M., 1999, Accumulation of polychlorinated biphenyls by the infaunal brittle starts *Amphiura filiformis* and *A. chiajei*: effects of eutrophication and selective feeding. *Mar Ecol Prog Ser* **186**, 173-185.

Gustafsson, Ö., Gschwend, P.M., Buesseler, K.O., 1997. Settling removal rates of PCBs into the northwestern Atlantic derived from ^{238}U–^{234}Th desquilibria. Environ. Sci. Technol. **31**,3544–3550.

Hawker, D.W., Connel, D.W., 1985. Relationships between partition coefficient, uptake rate constant, clearance rate constant, and time to equilibrium for bioaccumulation. *Chemosphere* **14**, 1205-1219.

Hedges, J. I., Baldock, J. A., Gelinas, Y., Lee, C., Peterson, M. L. and Wakeham, S. G. 2002. The biochemical and elemental compositions of marine plankton: A NMR perspective. *Marine Chemistry* 78), 47-63.

Ilyna, T., Pohlmann, T., Lammel, G., Sündermann, J., 2006. A fate of transport ocean model for persistent organic pollutants and its application to the North Sea. *J. of Mar. Systems* **63**,1–19.

Jassby, A. D. and Platt, T. 1976. Mathematical formulation of the relationship between photosynthesis and light for phytoplankton. *Limnol. Oceanogr.* **21**, 540-547.

Jaward, F. M., Barber, J. L., K. Booij, J. Dachs, R. Lohmann and K. C. Jones. 2004. Evidence ofr dynamic air-water coupling and cycling of persistent organic pollutants over the open Atlantic Ocean. *Environ. Sci. Technol.* **38**, 2617-2625.

Jurado, E. Jaward, F. M. Lohmann, R. Jones, K. C. Simo, R. Dachs, J. 2004. Atmospheric Dry Deposition of Persistent Organic Pollutants to the Atlantic and Inferences for the Global Oceans. *Environ. Sci. Technol.* **38**: 5505-5513.

Jurado, E., Jaward, F., Lohmann, R., Jones, K. C., Simo, R and Dachs, J, 2005. Wet deposition of persistent organic pollutants to the global oceans. *Environ. Sci. Technol.* **39**, 2426-2435.

Jurado, E., Zaldivar, J.M., Marinov, D. and Dachs, J. 2007. Fate of persistent organic pollutants in the water column: Does turbulent mixing matter? *Ma. Poll. Bull.* **54**, 441-451.

Ko, F.-C., Sanford, L.P., Baker, J.E., 2003. Internal recycling of particle reactive organic chemicals in the Chesapeake Bay water column.*Marine Chemistry* **81**, 163–176.

Lancelot, C., J. Staneva, D. Van Eeckhout, J.M. Beckers & E. Stanev, 2002. Modelling the Danube-influenced north-western continental shelf of the Black Sea. II. Ecosystem response to changes in nutrient delivery by the Danube river after its damming in 1972. Estuarine and Coastal Shelf Science 54, 473-499.

Leip A. and Lammel, G., 2004. Indicators for persistence and long-range transport potential as derived from multicompartment chemistry-transport modelling. *Environ. Pollution* **128,** 205-221.

Luyten, P.J., Jones, J.E., Proctor, R., Tabor, A., Tett, P. and Wild-Allen, K., 1999. COHERENS – A coupled Hydrodynamical-Ecological Model for Regional and Shelf Seas: User Documentation. *MUMM Report*, Management Unit of the Mathematical Models of the North Sea, pp 911.

Maciel, H and Zaldívar, J. M., 2005. An overview of chemical mixtures assessment and modelling in the aquatic environment. EUR report n° 21859. JRC, EC. pp. 71.

Mandalakis, M and Stephanou G.E. 2006. Atmospheric concentration characteristics and gas-particle partitioning of PCBs in a rural area of eastern Germany. *Environmental Pollution* (in press)

Mandalakis, M. and Stephanou, E. G., 2004. Wet Deposition of Polychlorinated Biphenyls in the Eastern Mediterranean. *Environ. Sci. Technol.*, 38, 3011-3018

Mandalakis, M., Apostolaki, M., Stephanou, E. G., 2005. Mass budget and dynamics of polychlorinated biphenils in the Eastern Mediterranean Sea, *Global Biogeochemical cycles*, 19, GB3018, 1-16

Marinov, D., Dueri, S., Puillat, I., Zaldivar, J.M., Jurado, E. and Dachs, J. 2007- Description of contaminant fate model structure, functions, input data, forcing functions and physicochemical properties data for selected contaminants (PCBs, PAHs, PBDEs, PCDD/Fs) - EUR Report n 22627 EN.

Meijer, S.N., Dachs, J., Ferna´ndez, P., Camarero, L., Catalan, J., Del Vento, S., Van Drooge, B.L., Jurado, E., Grimalt, J.O., 2006. Modelling the dynamic air–water–sediment coupled fluxes and occurrence of polychlorinated biphenyls in a high altitude lake. *Environ. Poll.* **140**, 546–560.

Nelson, E. D.; McConnell, L. L.; Baker, J. E., 1998. Diffusive Exchange of Gaseous Polycyclic Aromatic Hydrocarbons and Polychlorinated Biphenyls across the Air-Water Interface of the Chesapeake Bay, *Environ. Sci. Technol.*, **32**, 912-919.

Oguz , T., Ducklow, H. W., Malanotte-Rizzoli, P., Murray, J. W., Shushkina, E. A., Vedernikov, V. I. and Unluata, U. 1999. A physical-biochemical model of plankton productivity and nitrogen cycling in the Black Sea. *Deep-Sea Res.* I **46**, 597-636.

Opperhuizen, A., 1991. Bioconcentration and biomagnification: is a distinction necessary. In: Nagel, R., Loskill, R. (Eds.), Bioaccumulation in Aquatic Systems. VCH Publishers, Weinheim, pp. 67-80.

Paasivirta, J., Sinkkonen, S., Mikkelson, P., Rantio, T. and Wania, F., 1999. Estimation of vapor pressures, solubilities and Henry's laws constants of selected persistent organic pollutants as functions of temperature. *Chemosphere* **39**, 811-832.

Regione Emilia Romagna, 2003, Zone vulnerabili da prodotti fitosanitari-Relazione Generale.

Russell, R.W, Gobas, F.A.P.C., Haffner, G.D., 1999. Role of chemical and ecological factors in trophic transfer of organic chemicals in aquatic food webs. *Environ. Toxicol. Chem*. **18**, 1250-1257.

Scheringer, M., Stroebe, M., Wania, F., Wegmann, F., Hungerbu¨ hler, K., 2004. The effect of export to the deep sea on the long-range transport potential of persistent organic pollutants. Environmental *Science and Pollution Research* **11** , 41–48.

Scheringer, M., Wegmann, F., Fenner, K., Hungerbühler, K., 2000.Investigation of the cold condensation of persistent organic pollutants with a global multimedia fate model. *Environ. Sci. Technol.* **34**, 1842–1850

Schulz-Bull, D.E., Petrick, G., Duinker, J.C., 1988. Chlorinated biphenyls in North Atlantic surface and deep water. *Mar. Poll. Bull.* **19**, 526–531.

Schulz-Bull, D.E., G. Petric, H. Johannsen, J.C. Duinker, 1997. Chlorinated biphenyls and *p,p'*-DDE in Mediterranean surface waters. *Croatica Chemica Acta*, 70(1), 309-321.

Schwarzenbach, R. P., Gschwend, P. M., Imboden, D. M., 2003, Environmental Organic Chemistry, 2nd Edition, Wiley Interscience, New York.

Sijm, D.T.H.M., Seinen, W., Opperhuizen, A., 1992. Life-cycle biomagnification study in fish. *Environ. Sci. Technol*. **26**, 2162-2174.

Skoglund, R.S. K. Stange, and D.L. Swackhamer. 1996. A kinetics model for predicting the accumulation of PCBs in phytoplankton. *Environ Sci Technol* **30**, 2113–2120.

Stange, K. and Swackhamer, D. L. 1994. Factors affecting phytoplankton species-specific differences in accumulation of 40 polychlorinated biphenyls (PCBs). *Environ. Toxicol. Chem*. **11**, 1849-1860.

Steele, J. H. and Henderson, E. W. 1992. The role of predation in plankton models. *J. of Plankton Res.* **14**, 157-172.

Swackhamer, D.L. and R.S. Skoglund. 1993. Bioaccumulation of PCBs by phytoplankton: kinetics vs. equilibrium. *Environ Toxicol Chem* **12**, 831-838.

Thomann R.V., 1989. Bioaccumulation model of organic chemical distribution in aquatic food chains. *Environ. Sci.Technol*. **23**, 699–707.

Thomann, R.V., Conolly, J.P., Parkerton, T.F., 1992. An equilibrium model of organic chemical accumulation in aquatic food webs with sediment interaction. *Environ. Toxicol. Chem*. **11**, 615-629.

Tolosa, I., Readman, J.W., Fowler, S.W., Villeneuve, J.P., Dachs, J., Bayona, J.M., Albaiges, J., 1997. PCBs in the western Mediterranean. Temporal trends and mass balance assessment. *Deep-Sea Research* II **44**, 907–928

Tsapakis, M. and Stephanou, E. G., 2005. Polycyclic Aromatic Hydrocarbons in the Atmosphere of the Eastern Mediterranean. *Environ. Sci. Technol.*; 39, 6584-6590.

Tsapakis, M., Apostolaki, M., Eisenreich, S., Stephanou, E. G., 2006. Atmospheric Deposition and Marine Sedimentation Fluxes of Polycyclic Aromatic Hydrocarbons in the Eastern Mediterranean Basin. *Environ. Sci. Technol.*, 40, 4922-4927.

Valino, J. J., 2000. Improving marine ecosystem models: Use of data assimilation and mecososm experiments. *J. Mar. Res*. **58**, 117-164.

Van der Oost R., J. Beyer , N. P.E. Vermeulen, 2003. Fish bioaccumulation and biomarkers in environmental risk assessment: a review. *Environmental Toxicology and Pharmacology* **13**, 57/149.

Vermeulen, N.P.E., 1996. Role of metabolism in chemical toxicity. In: Ioannides, C. (Ed.), *Cytochromes P450: Metabolic and Toxicological Aspects*. CRC Press, Boca Raton, FL, USA, 29-53.

Vigano, L., S. Galassi and A. Arillo, 1994. Bioconcentration of polychlorinated biphenyls (PCBs) in rainbow trout caged in the river Po. *Ecotoxicol. Environ. Safe*. **28**, 287-297.

Wallberg, P. and Andersson, A. 1999. Determination of adsorbed and absorbed polychlorinated biphenyls (PCBs) in seawater microorganisms. *Marine Chemistry* **64**, 287-299 .

Wania, F., Mackay, D., 1996. Tracking the distribution of persistent organic pollutants. E*nviron. Sci. Technol.* **30**, 390A–396A.

Wroblewski, J.A. 1977. A model of phytoplankton bloom formation during variable Oregon upwelling. *J. Mar. Res*. **35**, 357-394.

Zaldívar, J. M., Cattaneo, E., Plus, M., Murray, C. N., Giordani. G. and Viaroli, P., 2003, Long-term simulation of main biogeochemical events in a coastal lagoon: Sacca di Goro(Northern Adriatic Coast, Italy). *Continental Shelf Research* **23**, 1847-1876.

European Commission

EUR 22882 EN – Joint Research Centre
Title: **Integrated modeling of fate and effects of Persistent Organic Pollutants in Marine ecosystems**
Author(s): J. M. Zaldívar, D. Marinov, S. Dueri, I. Puillat, R. Carafa, N. Berrojalbiz, S. Lacorte E. Jurado and J. Dachs
Luxembourg: Office for Official Publications of the European Communities
2007 – 47 pp. – 21 x 29,7 cm
EUR – Scientific and Technical Research series – ISSN 1018-5593
ISBN 978-92-79-06662-7

Abstract
In this report, an integrated model including fate of contaminants and ecological models it is presented. The model has been developed for analysing the effects of contaminants at ecosystem level. The fate model was already presented in a previous report where it was implemented for the major families of POPs: PCDD/Fs, PCBs, PAHs and PBDEs. In this work an ecological model has been incorporated into the fate model and coupled with it in terms of organic matter. The model allows estimating the environmental concentrations of POPs and the main fluxes between compartments, i.e. air/water/sediments and organisms. In addition the model has been validated for PAHs based on experimental data available in literature and it is now used to analyse NERI's mesocosm experiments, where combined effects of nutrients and contaminants are assessed. Furthermore, the model is being validated with other contaminants families as the experimental results from Mediterranean campaigns are starting to be available.

The mission of the JRC is to provide customer-driven scientific and technical support for the conception, development, implementation and monitoring of EU policies. As a service of the European Commission, the JRC functions as a reference centre of science and technology for the Union. Close to the policy-making process, it serves the common interest of the Member States, while being independent of special interests, whether private or national.

LB NA 22882 EN C

ISBN 978-92-79-06662-7